Title

Changes in O-Linked N-Acetylglucosamine (O-GlcNAc) Homeostasis Activate the p53 Pathway in Ovarian Cancer Cells*

Journal

Journal of Biological Chemistry, 291(36)

ISSN

0021-9258

Authors

de Queiroz, Rafaela Muniz
Madan, Rashna
Chien, Jeremy
et al.

Publication Date

2016-09-01

DOI

10.1074/jbc.m116.734533

Peer reviewed

THE JOURNAL OF BIOLOGICAL CHEMISTRY VOL. 291, NO. 36, pp. 18897–18914, September 2, 2016

Changes in *O*-Linked *N*-Acetylglucosamine (*O*-GlcNAc) Homeostasis Activate the p53 Pathway in Ovarian Cancer Cells*

Received for publication, April 23, 2016, and in revised form, June 17, 2016 Published, JBC Papers in Press, July 11, 2016, DOI 10.1074/jbc.M116.734533

Rafaela Muniz de Queiroz[‡], Rashna Madan[§], Jeremy Chien[¶], Wagner Barbosa Dias[‡1], and Chad Slawson[‖2]

From the [‡]Laboratório de Glicobiologia Estrutural e Funcional, Instituto de Biofísica Carlos Chagas Filho, Centro de Ciências da Saúde, Universidade Federal do Rio de Janeiro, Cidade Universitária, Rio de Janeiro, 21941-902RJ, Brazil, the Departments of [‖]Biochemistry and Molecular Biology and [¶]Cancer Biology and [§]Division of Hematology/Oncology, Department of Pathology, University of Kansas Medical Center, Kansas City, Kansas 66160

O-GlcNAcylation is a dynamic post-translational modification consisting of the addition of a single *N*-acetylglucosamine sugar to serine and threonine residues in proteins by the enzyme *O*-linked β-*N*-acetylglucosamine transferase (OGT), whereas the enzyme *O*-GlcNAcase (OGA) removes the modification. In cancer, tumor samples present with altered *O*-GlcNAcylation; however, changes in *O*-GlcNAcylation are not consistent between tumor types. Interestingly, the tumor suppressor p53 is modified by *O*-GlcNAc, and most solid tumors contain mutations in p53 leading to the loss of p53 function. Because ovarian cancer has a high frequency of p53 mutation rates, we decided to investigate the relationship between *O*-GlcNAcylation and p53 function in ovarian cancer. We measured a significant decrease in *O*-GlcNAcylation of tumor tissue in an ovarian tumor microarray. Furthermore, *O*-GlcNAcylation was increased, and OGA protein and mRNA levels were decreased in ovarian tumor cell lines not expressing the protein p53. Treatment with the OGA inhibitor Thiamet-G (TMG), silencing of OGA, or overexpression of OGA and OGT led to p53 stabilization, increased nuclear localization, and increased protein and mRNA levels of p53 target genes. These data suggest that changes in *O*-GlcNAc homeostasis activate the p53 pathway. Combination treatment of the chemotherapeutic cisplatin with TMG decreased tumor cell growth and enhanced cell cycle arrest without impairing cytotoxicity. The effects of TMG on tumor cell growth were partially dependent on wild type p53 activation. In conclusion, changes in *O*-GlcNAc homeostasis activate the wild type p53 pathway in ovarian cancer cells, and OGA inhibition has the potential as an adjuvant treatment for ovarian carcinoma.

O-GlcNAcylation is an abundant, dynamic, and inducible post-translational modification (PTM)[3] similar to phosphorylation. This PTM is characterized by addition of an *N*-acetylglucosamine (GlcNAc) from the precursor UDP-GlcNAc to serine and threonine residues on proteins (1). The addition of *O*-linked β-*N*-acetylglucosamine (*O*-GlcNAc) to proteins is catalyzed by *O*-GlcNAc transferase (OGT), whereas *O*-GlcNAcase (OGA) catalyzes its removal (2). Unlike extracellular glycosylation, *O*-GlcNAc is not elongated into more complex structures and is localized mainly in nucleocytoplasmic compartments (3). *O*-GlcNAcylation modulates protein functions such as enzymatic activity, protein degradation, protein-protein interaction, subcellular localization, and transcriptional activity (4). *O*-GlcNAcylation plays an important role in cellular function because deletion of OGT is lethal in developing animals and in tissue culture (5). Changes in *O*-GlcNAcylation impact many cellular processes like cell cycle progression (6), kinase activation (7), and gene transcription (8).

Like most post-translational modifications, *O*-GlcNAcylation can alter the function, stability, or localization of a protein. For example, increases in *O*-GlcNAcylation alter the function of the calcium/calmodulin-dependent kinase IV via *O*-GlcNAc residues competing with phosphorylation at a key activation site (7). Interestingly, *O*-GlcNAc appears to act as a sensor of the cellular environment. The basal balance between addition and removal of *O*-GlcNAc in a cell is called *O*-GlcNAc homoeostasis, and disruption of this homeostasis is seen in many pathological (3) and non-pathological (9) conditions such as in response to different stress inputs (10). Disruption in basal *O*-GlcNAc homeostasis correlates with pathologies like Alzheimer disease, metabolic syndrome, and cancer (11).

Cancer cells exhibit important metabolic differences from normal cells known as the Warburg effect. This phenomenon is characterized by a high rate of glycolytic flux and increased glucose uptake by tumor cells (12). The higher activity of the glycolytic pathway coupled with an increase in glucose uptake occurs in several types of human cancers. Importantly, glucose feeds into the hexosamine biosynthetic pathway (HBP), a branch of glucose metabolism responsible for the synthesis of UDP-GlcNAc, the metabolic substrate for OGT (13). Several HBP genes are overexpressed in human prostate cancers (14) suggesting that cancer cells have increased flux through the HBP. More metabolite flux through the HBP increases

* This work was supported by National Institutes of Health Grant R01DK100595 from NIDDK (to C. S.), Conselho Nacional de Desenvolvimento Científico e Tecnológico (CNPq) (to R. M. d. Q. and W. B. D.), by Fundação Carlos Chagas Filho de Amparo à Pesquisa do Estado do Rio de Janeiro (FAPERJ) (to W. B. D.), and by Department of Defense Grant W81XWH-10-1-0386 (to J. C.). The authors declare that they have no conflicts of interest with the contents of this article. The content is solely the responsibility of the authors and does not necessarily represent the official views of the National Institutes of Health.

[1] To whom correspondence may be addressed. E-mail: diaswb@biof.ufrj.br.
[2] To whom correspondence may be addressed. E-mail: cslawson@kumc.edu.

[3] The abbreviations used are: PTM, post-translational modification; OGT, *O*-linked β-*N*-acetylglucosamine transferase; OGA, *O*-GlcNAcase; TMG, Thiamet-G; HBP, hexosamine biosynthetic pathway; qPCR, quantitative PCR; GFAT, glutamine-fructose-6-phosphate-aminotransferase; PI, propidium iodide; MTT, 3-(4,5-dimethylthiazol-2-yl)-2,5-diphenyltetrazolium bromide.

the levels of UDP-GlcNAc providing more substrate for *O*-GlcNAcylation (15).

Indeed, the levels of *O*-GlcNAc and protein expression of OGT and OGA are aberrant in different tumors and may be associated with prognosis and tumor grade (3). However, there is not a clear pattern of *O*-GlcNAcylation changes between different tumor types. In lung and colon cancer, for example, there is an increase in *O*-GlcNAcylation and OGT levels compared with normal tissue (16). However, in thyroid cancer *O*-GlcNAc levels are lower and OGA activity is higher when compared with normal thyroid tissue (17). *O*-GlcNAcylation was proposed as a prognostic factor for prostate cancer and leukemia with high *O*-GlcNAc levels in leukemia patients leading to a better prognosis (18); however, in prostate cancer higher *O*-GlcNAc correlates with a poor prognosis (19). All these conflicting data show that *O*-GlcNAc can have different roles in different tissues, contributing to or impairing tumor development and treatment. However, one thing is common to all tumor types tested, alterations in *O*-GlcNAcylation are reported in cell transformation (20). Nevertheless, questions about the functional role of these *O*-GlcNAc changes in the acquisition of malignancy and tumor progression still remain.

During cell transformation, many signaling pathways become deregulated due to a gain of function of oncogenes and a loss of function of tumor suppressors. The tumor suppressor p53 plays a critical role in cell biology, controlling functions such as cell cycle progression, DNA damage response, apoptosis, senescence, and angiogenesis (21). Under normal conditions, p53 is ubiquitinated by the E3-ubiquitin ligase Mouse Double Minute 2 homolog (MDM-2) causing the continual degradation of p53 through the proteasome (22). However, in response to stress, p53 is stabilized and activated by PTMs that inhibit its interaction with MDM-2 and promote interactions with co-factors and DNA leading to the up-regulation of genes related to stress response and cell cycle arrest (23). In cancer, p53 is found silenced or mutated in 50–55% of the all cases losing its function as a tumor suppressor (24). Mutations in p53 also correspond to poor prognosis and low response to chemotherapy (25).

Previously, p53 was found to be *O*-GlcNAcylated at Ser-149. *O*-GlcNAcylation of p53 led to a decrease in p53 degradation by the proteasome suggesting that *O*-GlcNAc stabilizes p53 (26). However, very little is known about the consequences of altered *O*-GlcNAc homeostasis and its effects on the p53 pathway. The aim of this work is to study the relationship between *O*-GlcNAc and ovarian cancer and to understand the connection between *O*-GlcNAcylation and p53 because ovarian cancer has a high p53 mutation rate (27). Our data reveal that wild type p53 senses changes in cellular *O*-GlcNAcylation to modulate gene transcription and suggests OGA inhibition as a potential target for adjuvant therapy in cancer.

Results

O-GlcNAcylation Is Decreased in Ovarian Tumors Compared with Normal Tissue—Changes in *O*-GlcNAcylation levels as well as OGT and OGA expression occur with cellular transformation (3); however, no clear diagnostic or prognostic pattern has emerged between normal and tumor tissue. Using a tumor microarray containing 48 ovarian tumors samples and nine normal tissue samples, we evaluated the changes in *O*-GlcNAcylation, OGT, and OGA between normal and cancer tissue. The tissue microarray contained two different sets of patient samples as follows: the first set consists of patient-matched primary tumor and recurrent tumors, and the second set contains patient-matched primary and metastatic carcinoma samples. The scores generated by the staining intensity were compared within and across these groups. We found that in all groups *O*-GlcNAcylation in the cytoplasm was very low with higher amounts of *O*-GlcNAcylation occurring in the nucleus. OGT expression was predominantly nuclear, whereas OGA expression was distributed between the cytoplasm and nucleus. *O*-GlcNAcylation was significantly decreased in tumor tissue when compared with normal tissue, and no significant difference was found between primary and recurrent tumors or primary and metastatic tumors (Fig. 1, *A*–*D*). No significant differences were found comparing tumor grades or tumor phenotypes (data not shown). In ovarian tumors, OGA expression is significantly decreased in the cytoplasm with a slight but not significant increase in the nucleus (Fig. 1, *C* and *D*). OGT expression in tumor tissues is significantly decreased in the nucleus with a slight but not significant increase in the cytoplasm (Fig. 1, *C* and *D*). These data indicate that ovarian tumors present with less *O*-GlcNAcylated proteins than normal ovary tissue, with decreased OGA cytoplasmic expression and increased OGT nuclear expression.

O-GlcNAcylation Is Related to the Presence but Not the Transcriptional Activity of p53—To investigate the relationship between *O*-GlcNAcylation and p53 status, we used five cell lines with different p53 backgrounds. We used ovarian cell lines A2780 (wild-type p53), SKOV-3 (p53 null), OVCAR-7 (p53 null), OVCAR-8 (splice variant), and OVCAR-10 (one allele mutated, point mutation) (Table 1). A2780, OVCAR-10, and OVCAR-8 express p53, whereas SKOV-3 and OVCAR-7 do not produce the protein (Fig. 2*A*). All cell lines except p53 null SKOV-3 produce p53 transcripts (Fig. 2*B*). Expression of p53-target genes, CDKN1 (p21) and BAX, are low in all cells in comparison with p53 wild type cell line A2780. (Fig. 2*C*).

Next, we analyzed the overall *O*-GlcNAcylation status as well as expression of OGA, OGT, and glutamine-fructose-6-phosphate-aminotransferase (GFAT), the key enzyme in the production of UDP-GlcNAc, the metabolic substrate for OGT. *O*-GlcNAcylation, OGA, OGT, and GFAT protein expression were unrelated to mutations in the p53 gene, *TP53* (Fig. 3, *A* and *B*). Gene expressions of MGEA5 (OGA), OGT, GFPT1 (GFAT1), and GFPT2 (GFAT2) were also unrelated to mutations in TP53 (Fig. 3*C*). Curiously, OGT mRNA was significantly elevated in the OVCAR-10 cell line; however, this mRNA change did not correlate with protein level (Fig. 3, *A*–*C*). Interestingly, OGA protein and mRNA levels are higher, accompanied by decrease in *O*-GlcNAcylation in cells with p53 protein expression (Fig. 3, *A*–*C*). Furthermore, p53 chromatin immunoprecipitation (ChIP) data showed no binding of p53 at the OGA or OGT promoter[4] in two p53 wild type tumor cell lines

[4] J. Chien, unpublished data.

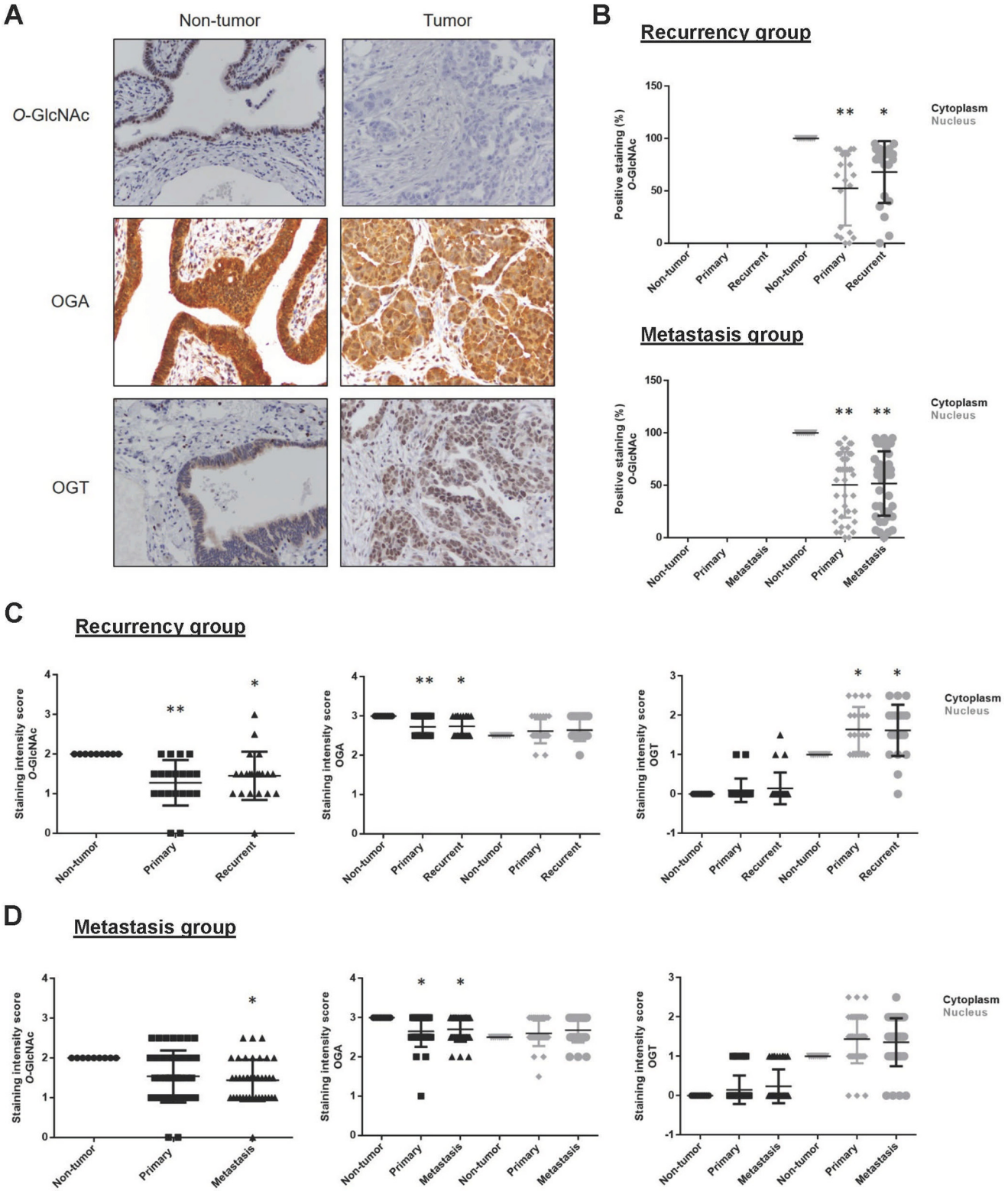

FIGURE 1. ***O*-GlcNAcylation is lower in ovarian cancer *in vivo*.** Tissue microarray analysis was performed by immunochemistry staining of patient samples. *A,* representative micrographs of immunostaining for *O*-GlcNAc, OGA, and OGT in normal and tumor tissue samples (×20 magnification). *B,* analyses of percentage of positivity for *O*-GlcNAc in different sample groups. *C* and *D,* analyses of Score Intensity Staining for overall *O*-GlcNAc and OGA and OGT in the nucleus and cytoplasm in different sample groups. The Score Intensity Staining was classified as absent (0), weak (1), moderate (2), and strong (3). *, $p < 0.05$; **, $p < 0.01$; ***, $p < 0.0001$.

(RMG1 and TOV21G). These data suggest that OGA expression and *O*-GlcNAcylation are related to the presence of p53, but not necessarily to p53 function as a transcription factor.

O-GlcNAc Regulates Wild Type p53 Stability and Activity—Because *O*-GlcNAc regulates p53 stability (26), we asked the question whether changes in cellular *O*-GlcNAc levels influ-

TABLE 1
Overview of TP53 gene alterations in cancer cell lines
Hm means homozygosity. Ht means heterozygosity. ATCC means American Type Culture Collection.

Cell line	DNA mutational profile	Refs.
A2780	Wild type	Anglesio *et al.* (51)
SKOV-3	S90fs*33 (Hm)	ATCC database
OVCAR-7	Not verified	
OVCAR-8	126–132 del (Hm)	Anglesio *et al.* (51)
OVCAR-10	V172F (Ht)	Zhang *et al.* (52)

ence p53 activity. First, we used Thiamet-G (TMG), an OGA inhibitor, to increase overall *O*-GlcNAcylation (28). Treatment with TMG for 6 and 24 h had no significant effect on p53 or MDM-2 protein levels (Fig. 4*A*) or p53 mRNA levels (Fig. 4*C*). However, we did see an increase in mRNA levels of p53 target gene BAX and increased protein and mRNA levels of p21 (Fig. 4, *B* and *D*) in cell lines with functional p53. In cell lines with mutated p53, we saw no significant differences. A slight increase in p21 protein and mRNA levels did occur in OVCAR-8 (Fig. 4, *B* and *D*).

Transcription factors like p53 have to translocate to the nucleus and bind to the DNA to promote target gene transcription. Next, we analyzed p53 subcellular location in response to TMG treatment and OGA silencing. TMG treatment caused an increase in wild type p53 translocation to the nucleus (Fig. 4, *E* and *F*). However, mutant p53 localization was insensitive to TMG treatment (Fig. 4, *G* and *H*).

To confirm these results we produced stable A2780 cell lines silenced for OGA (Fig. 5*A*). Wild type p53 cells had increased mRNA levels of Bax, higher protein and mRNA levels of p21, but no changes in p53 levels when OGA was silenced (Fig. 5, *A–D*). OGA knockdown caused an increase in wild type p53 translocation to the nucleus (Fig. 5, *E* and *F*). These data suggest that modulation of OGA function either pharmacologically or by loss of the enzyme expression influences wild type p53 function.

Because pharmacological inhibition and loss of function of OGA altered p53 pathway function, we then decided to manipulate *O*-GlcNAc levels by overexpressing either OGT or OGA (Fig. 6*A*). We found a significant increase in wild type p53 protein levels when OGA or OGT was overexpressed (Fig. 6, *B* and *C*). Interestingly, OGA/OGT overexpression increased the protein levels of all major p53 isoforms (p53α, p53β, and p53γ) (Fig. 6, *B* and *C*). Protein expression of p53 target genes p21 and MDM-2 (Fig. 6, *B* and *C*) as well as mRNA levels p21 and BAX (Fig. 6, *D* and *E*) were higher in these cells. However, p53 and p53 isoforms of mRNA expression were not increased by OGA or OGT overexpression (Fig. 6, *D* and *E*, data not shown). We also analyzed the effect of OGA and OGT overexpression in the p53-mutated cell line OVCAR-8. No difference in p53 or p21 levels was observed in OVCAR-8 cells (Fig. 6*B*). Still, to determine whether this phenomenon is dependent on wild type p53 and not specific to ovarian cancer cells, we overexpressed OGA and OGT in wild type p53 neuroblastoma SH-SY5Y cells. Overexpression of both enzymes in SH-SY5Y also led to increased p53 and p21 levels (Fig. 6*B*). As with the TMG treatment, we measured increased p53 nuclear translocation in OGA- and OGT-overexpressing cells (Fig. 6, *F* and *G*). These data suggest that overexpression of OGA and OGT led to stabilization, nuclear accumulation, and activation of wild type p53. Interestingly, OVCAR-8 cells, which have mutated p53, do not show p53 stabilization in response to OGA nor OGT overexpression.

O-GlcNAcylation Influences Post-translational Modifications of the p53 Pathway—Several PTMs such as phosphorylation, acetylation, ubiquitination, and methylation can regulate p53 function (23). Importantly, p53 is *O*-GlcNAcylated at Ser-149, and this modification is related to stability of the protein (26). Because increased *O*-GlcNAc levels generated by TMG treatment led to activation of p53, we hypothesized this effect was due to increased p53 *O*-GlcNAcylation. A2780 cells overexpressing p53-GFP fusion protein were treated with TMG for 4 h. Immunoprecipitation of p53 was performed and then probed for *O*-GlcNAcylation. *O*-GlcNAcylated p53 in this cell line was undetectable even after p53 overexpression and inhibition of OGA (Fig. 7*A*). These data suggest that changes in p53 levels and activation caused by treatment with TMG or OGA/OGT overexpression were likely not due to p53 *O*-GlcNAcylation.

MDM-2 levels control the stability of p53. Phosphorylation of MDM-2 at Ser-166 is responsible for preventing MDM-2 ubiquitination and degradation (29) leading to increased MDM-2 cytoplasmic levels and decreasing p53 levels. Interestingly, overexpression of OGA and OGT significantly increased MDM-2 phosphorylation at Ser-166 (Fig. 7*B*).

Once p53 is stabilized, it translocates to the nucleus to activate transcription of target genes. The ability of p53 to bind DNA and induce transcription is controlled by other PTMs such as acetylation. Acetylation of p53 increases p53 binding to promoters and correlates with increased p53 activity (23). Using a specific antibody to acetylated p53 at Lys-382, we measured increased p53 acetylation after OGT overexpression and OGA silencing (Fig. 7*C*). When normalized to p53 expression, the increase in acetylation of p53 was higher after OGT overexpression and in OGA knockdowns. Importantly, OGA/OGT overexpression did not alter protein levels of the enzymes responsible for p53 Lys-382 acetylation (p300) and deacetylation (Sirt1) (Fig. 7*D*). The results suggest that increased *O*-GlcNAc levels enhance acetylation of p53 in lysine 382, but the changes do not occur through modulation of p300 or Sirt1 protein levels.

TMG Treatment Impairs Tumor Cell Growth without Altering Cisplatin Cytotoxicity—The major function of p53 in cells is as a tumor suppressor. Because *O*-GlcNAc modulation increases p53 stabilization and activity, we hypothesized that TMG treatment could improve the efficiency of a chemotherapeutic agent like cisplatin, a chemotherapeutic used in the clinic to treat ovarian cancer. We performed colony formation assays with cisplatin and TMG. We preincubated A2780 cells with or without TMG followed by 24 h of cisplatin treatment. Eleven days later, the number of colonies was analyzed. Cells preincubated with TMG formed significantly fewer colonies than cells in the absence of the inhibitor (Fig. 8, *A* and *B*). The IC_{50} value of cisplatin decreased more than 30% in cells preincubated with TMG (Fig. 8*B*). To determine whether the difference found was due to increased cytotoxicity, we performed cell viability assays but found no significant difference in cell viabil-

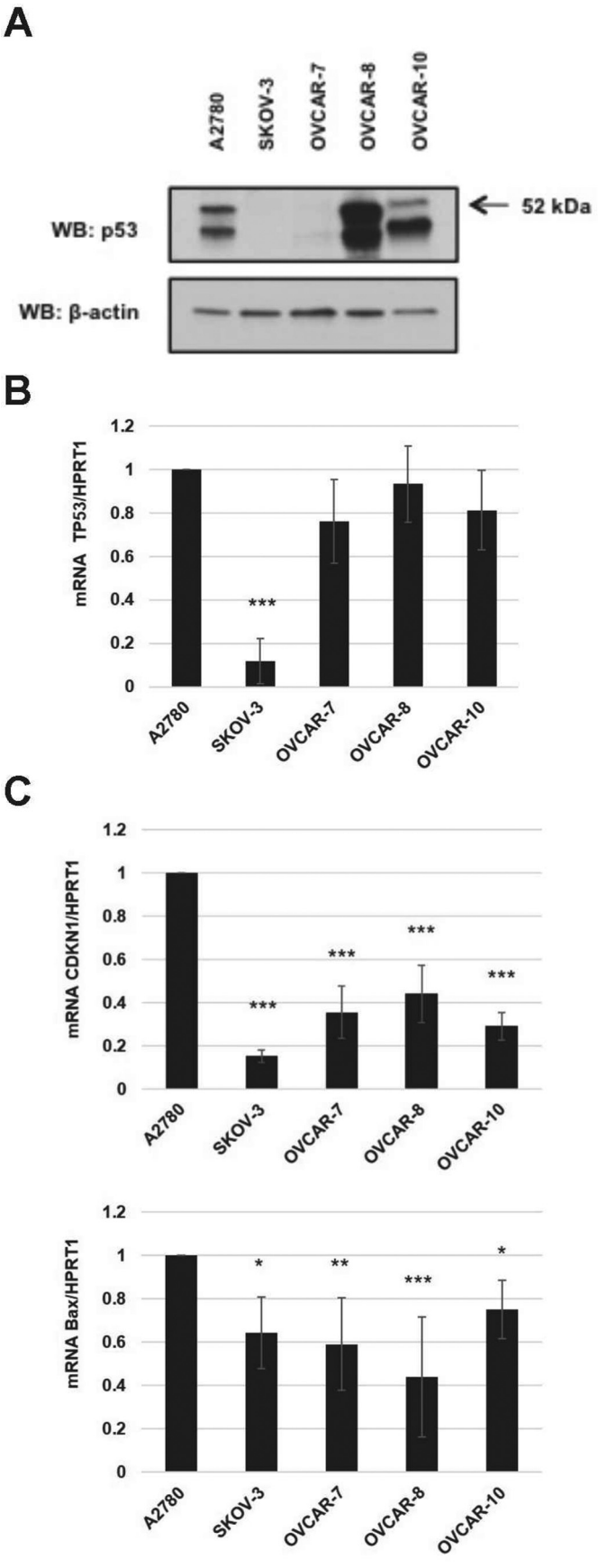

ity in the presence or absence of TMG (Fig. 8*C*). Corroborating these findings, we performed annexin PI staining and measured no significant differences in apoptosis induced by cisplatin in the presence or absence of TMG (Fig. 8*D*), nor did we measure changes in early or late apoptosis or induction of necrosis (Fig. 8*E*).

TMG Treatment Increases G_2/M Cell Cycle Arrest Induced by Cisplatin in a Partially p53-dependent Manner—Because reduction in colonies of A2780 cells after cisplatin and TMG treatment was not due to increased cell death, we suspected from previous work (6) that TMG would decrease cell growth. Combined with cisplatin, TMG treatment decreased protein levels of MDM-2 and increased levels of p21, a cell cycle inhibitory protein (Fig. 9, *A* and *B*) suggesting that p53 was more active in cells treated with TMG. Using propidium iodide staining to analyze DNA content, we evaluated the cell cycle phases before and after cisplatin treatment in the presence or absence of TMG. TMG alone did not interfere with cell cycle progression (Fig. 9*C*). However, cells exposed to TMG and then treated with cisplatin for 24 h had significantly more cells arrested at G_2/M (Fig. 9, *C* and *D*) suggesting that TMG treatment decreased tumor cell growth by reducing cell cycle progression after cisplatin treatment without impairing cisplatin cytotoxic effects.

To analyze whether the effect of TMG on cell growth was due p53 pathway activation, we performed the colony formation assay in A2780 cells silenced for p53. TMG treatment significantly affected colony formation in p53 wild type cells (A2780 shCtr) treated with cisplatin, but when p53 was silenced in these cells (A2780 sh p53#1), the decrease in colony formation was no longer significant (Fig. 10, *A* and *B*). These data suggest that the effects of TMG on cell growth during cisplatin treatment were partially dependent on wild type p53 pathway activation.

Discussion

The control of cell death and cell growth by the p53 pathway is key for cellular homeostasis and tumor suppression. Defects in p53 pathway activation are intrinsically related to cell malignancy (30) and tumor development (31). Given that high grade serous ovarian cancer has one of the highest p53 mutation rates (32), we investigated the relationship between the p53 pathway and *O*-GlcNAcylation. Our results revealed a significant decrease in *O*-GlcNAcylation in ovarian tumors compared with normal tissues. Next, we showed in ovarian cell lines expressing wild-type p53 that pharmacological inhibition of OGA, silencing of OGA, or overexpression of OGA or OGT increased wild type p53 stability, translocation, and activation, although we observed no stabilization effect in cell lines with mutated p53. Finally, treatment with cisplatin combined with TMG

FIGURE 2. **Characterization of p53 status in ovarian cancer cell lines.** *A,* p53 protein levels were measured by immunoblot in five ovarian cancer cell lines. Actin was used as a loading control. *B,* p53 mRNA levels (*TP53*) were measured in five cancer cell lines and normalized to HPRT1 (*HPRT1*) mRNA levels. *C,* mRNA levels of p53 target genes, p21 (*CDKN1*) and Bax (*BAX*), were analyzed in all cell lines and normalized to HPRT1. All experiments were performed with at least three biological replicates. *, $p < 0.05$; **, $p < 0.01$; ***, $p < 0.0001$; *WB*, Western blotting.

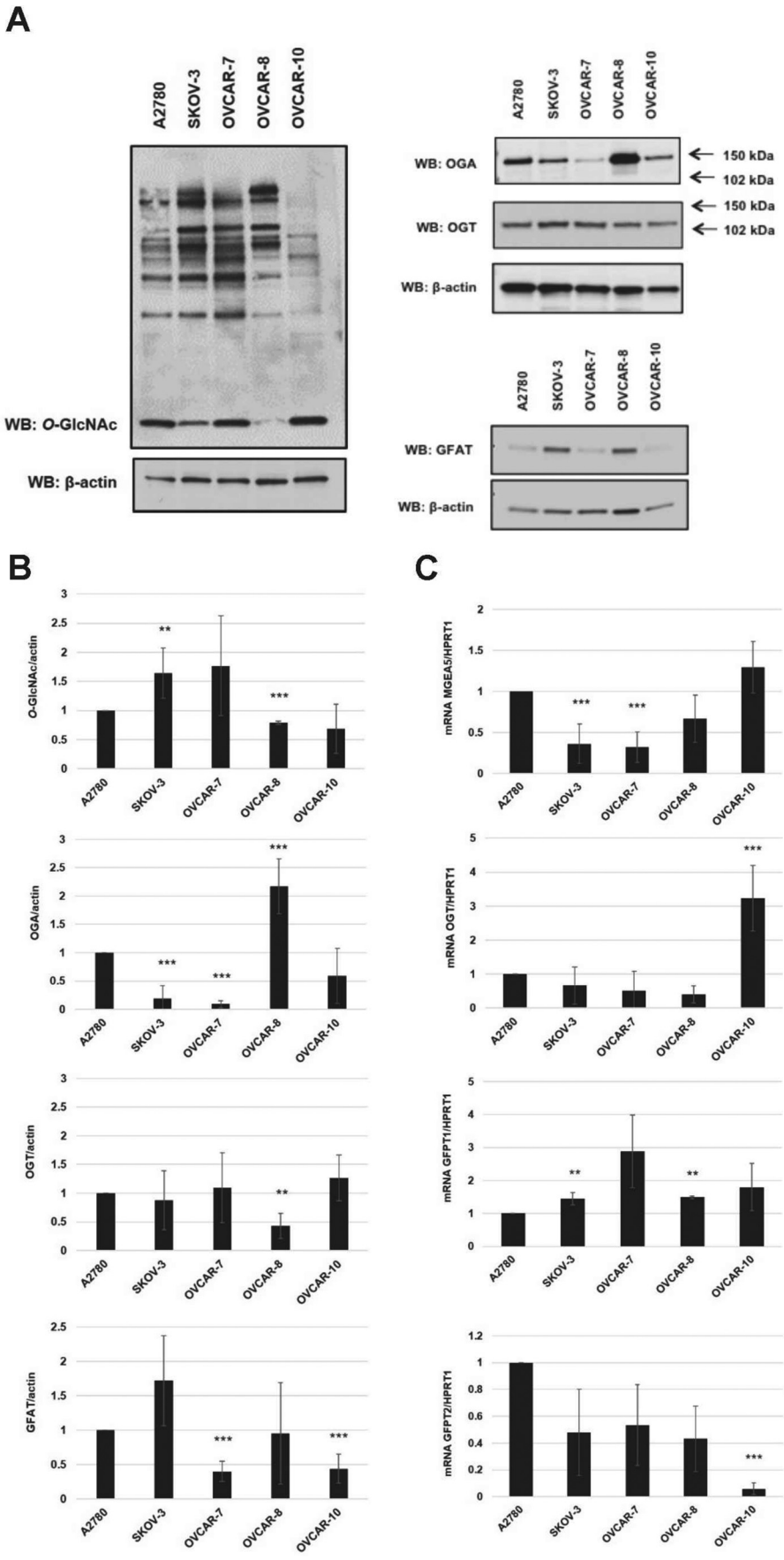
A
A2780
SKOV-3
OVCAR-7
OVCAR-8
OVCAR-10
WB: O-GlcNAc
WB: β-actin
WB: OGA
WB: OGT
WB: β-actin
150 kDa
102 kDa
150 kDa
102 kDa
WB: GFAT
WB: β-actin
B
O-GlcNAc/actin
OGA/actin
OGT/actin
GFAT/actin
C
mRNA MGEA5/HPRT1
mRNA OGT/HPRT1
mRNA GFPT1/HPRT1
mRNA GFPT2/HPRT1

enhanced cell cycle arrest at G_2/M, and this effect is partially dependent on activation wild-type p53.

Changes in *O*-GlcNAcylation levels commonly occur between normal and tumor tissue (3), but the changes do not follow a consistent pattern between tumors from different tissues. In this work, we saw a significant decrease of *O*-GlcNAcylation in ovarian tumor tissue. Expression of OGA was significantly decreased in the cytoplasm with a trend toward higher nuclear localization, whereas OGT showed a slight increase in cytoplasmic localization in the tumor samples. Importantly, OGT and OGA as essential genes in the human genome (33, 34) demonstrate the importance of *O*-GlcNAcylation for normal cellular function; therefore, we did not expect dramatic changes in OGT or OGA expression. The heterogeneity in the expression of *O*-GlcNAc, OGA, and OGT in cancer suggests diverse mechanisms regulating O-GlcNAcylation. However, ovarian cancer shows a significant decline in overall O-GlcNAcylation. In this study, we did not analyze differences in *O*-GlcNAcylation of specific proteins, but further studies are needed to investigate these potential changes.

Using five tumor cell lines with different p53 backgrounds, we showed higher levels of OGA protein expression and decreased *O*-GlcNAcylation in cell lines expressing wild type or mutant p53. These data suggest that OGA expression does not depend directly on p53 transcriptional activity. Although p53 is a known transcription factor, it also displays functions not related to gene transcription. Cytoplasmic p53 can induce apoptosis and necroptosis via mitochondrial permeabilization (35). Using a cytoplasmic p53 mutant, p53 inhibited autophagy though a non-nuclear effect (36). Thus, the changes in OGA expression could be a result of a cytoplasmic p53 effect on other intracellular pathways leading to a secondary effect on OGA expression and consequently *O*-GlcNAc levels.

Restoring the expression of wild type p53 is an approach in cancer therapy due to the fact that increased p53 will suppress tumor growth and promote cell death. The use of molecules that inhibit MDM-2 mediated destruction of p53, thereby stabilizing the tumor suppressor, showed encouragingly results in *in vitro*, animal, and patient studies (37, 38). Here, we show that modulation of *O*-GlcNAcylation results in stabilization of wild type p53 and activation of the p53 pathway in p53 wild type ovarian and neuroblastoma cancer cells. Other studies using mouse embryonic fibroblasts and mouse retinal pericytes investigated the correlation between *O*-GlcNAc changes and p53 levels, but none of them show effects on stabilization of p53 by *O*-GlcNAc (39–41). Interestingly, *O*-GlcNAc modulation did not increase p53 levels or translocation of p53 to the nucleus in the p53-mutated cell line OVCAR-8. Mutation of p53 generates loss of function of the protein and, in some cases, a gain of new functions such as increased invasion, genomic instability, and drug resistance (42). Thus, changes in *O*-GlcNAcylation would lead to activation of the tumor-suppressive pathway in p53 wild type cells but not the activation of the oncogenic pathway in p53 mutant cells. Although changes in *O*-GlcNAc had no effect on the p53 mutant found in OVCAR-8 cells, more studies are needed to establish whether different gain of function p53 mutants are affected by *O*-GlcNAc modulation.

Cells maintain a basal homeostatic level of *O*-GlcNAc. Changes in nutrient availability alter *O*-GlcNAc homeostasis leading to *O*-GlcNAc-mediated changes in cellular function (43). Furthermore, pharmacological inhibition or gain or loss of OGT and OGA expression alters *O*-GlcNAc homeostasis by disrupting *O*-GlcNAc cycling (43). Interestingly, stabilization and/or activation of p53 occurred after increasing (TMG treatment, OGT overexpression, and OGA knockdown) and decreasing (OGA overexpression) *O*-GlcNAc levels. Thus, p53 pathway activation occurs after any change in *O*-GlcNAc homeostasis suggesting that p53 acts as an *O*-GlcNAc homeostasis sensor. Increased *O*-GlcNAcylation occurs in response to many stress stimuli (10, 44), and changes in *O*-GlcNAc homeostasis may act as a stress signal triggering stress-response activation of the p53 pathway. Thus, modulation of *O*-GlcNAc levels would be an upstream signal triggering the p53 pathway activation in response to stress.

Post-translational modifications are a key step in activation of the p53 pathway (23). For example, p53 is *O*-GlcNAcylated at serine 149 resulting in decreased interaction with MDM-2, reduced ubiquitination of p53, and stabilization of the protein (26). In our results, we showed that disruption of *O*-GlcNAc homeostasis stabilized p53, but we were unable to measure *O*-GlcNAc on p53. Potentially, *O*-GlcNAcylated p53 in these cell lines compared with the MCF-7 cell line used previously to map the *O*-GlcNAc site is very low and not detectable. Furthermore, reduced *O*-GlcNAcylation caused by OGA overexpression increased p53 levels and activation. These data suggest that changes in the levels of *O*-GlcNAc on p53 are less critical to regulating p53 stability in A2780 cells then disrupting homeostatic levels of *O*-GlcNAc.

Acetylation of p53 correlates to increased DNA binding and transcriptional activity (23). Increased *O*-GlcNAcylation in OGT-overexpressing cells or OGA knockdowns increased acetylated p53 at lysine 382. This increase in the modification results in higher transcription of p53 target genes. For example, acute exposure of human umbilical vein endothelial cells to high glucose media increases acetylation of p53 and expression of p21 (45). The expression of the enzymes p300 and SIRT1 involved in Lys-382 acetylation and deacetylation, respectively (46), was altered in the human umbilical vein endothelial cells exposed to high glucose (45). In our ovarian cancer model, protein levels of both enzymes are unchanged after OGA and OGT overexpression; however, changes in *O*-GlcNAc homeostasis

FIGURE 3. ***O*-GlcNAcylation is not related to mutations on p53 gene.** *A*, *O*-GlcNAcylation levels, OGA, OGT, and GFAT protein levels were measured in all five cancer cell lines. Actin was used as a loading control. *B*, densitometry of *O*-GlcNAcylation OGA, OGT, and GFAT protein levels in each cell line normalized to actin. *C*, OGA (*MGEA5*), OGT (*OGT*), GFAT1 (*GFPT1*), and GFAT2 (*GFPT2*) mRNA levels were measured in all five cancer cell lines and normalized to HPRT1 mRNA levels. All experiments were performed with at least three biological replicates. *, $p < 0.05$; **, $p < 0.01$; ***, $p < 0.0001$; *WB*, Western blotting.

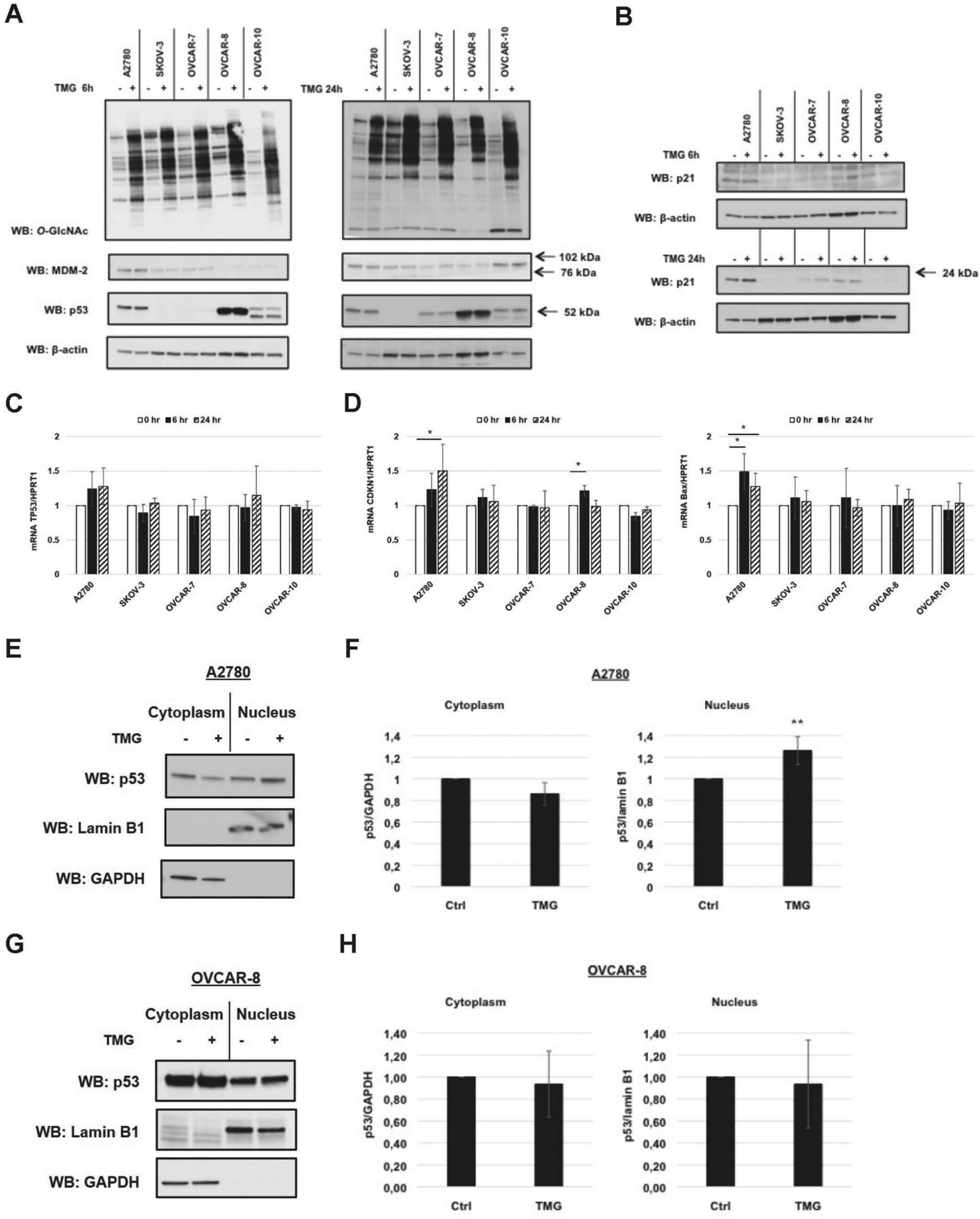
A
A2780
SKOV-3
OVCAR-7
OVCAR-8
OVCAR-10
TMG 6h
TMG 24h
WB: O-GlcNAc
WB: MDM-2
WB: p53
WB: β-actin
102 kDa
76 kDa
52 kDa
B
TMG 6h
WB: p21
WB: β-actin
TMG 24h
24 kDa
C
0 hr 6 hr 24 hr
mRNA TP53/HPRT1
D
mRNA CDKN1/HPRT1
mRNA Bax/HPRT1
E
A2780
Cytoplasm
Nucleus
TMG
WB: p53
WB: Lamin B1
WB: GAPDH
F
A2780
Cytoplasm
Nucleus
p53/GAPDH
p53/lamin B1
Ctrl
TMG
G
OVCAR-8
H
OVCAR-8

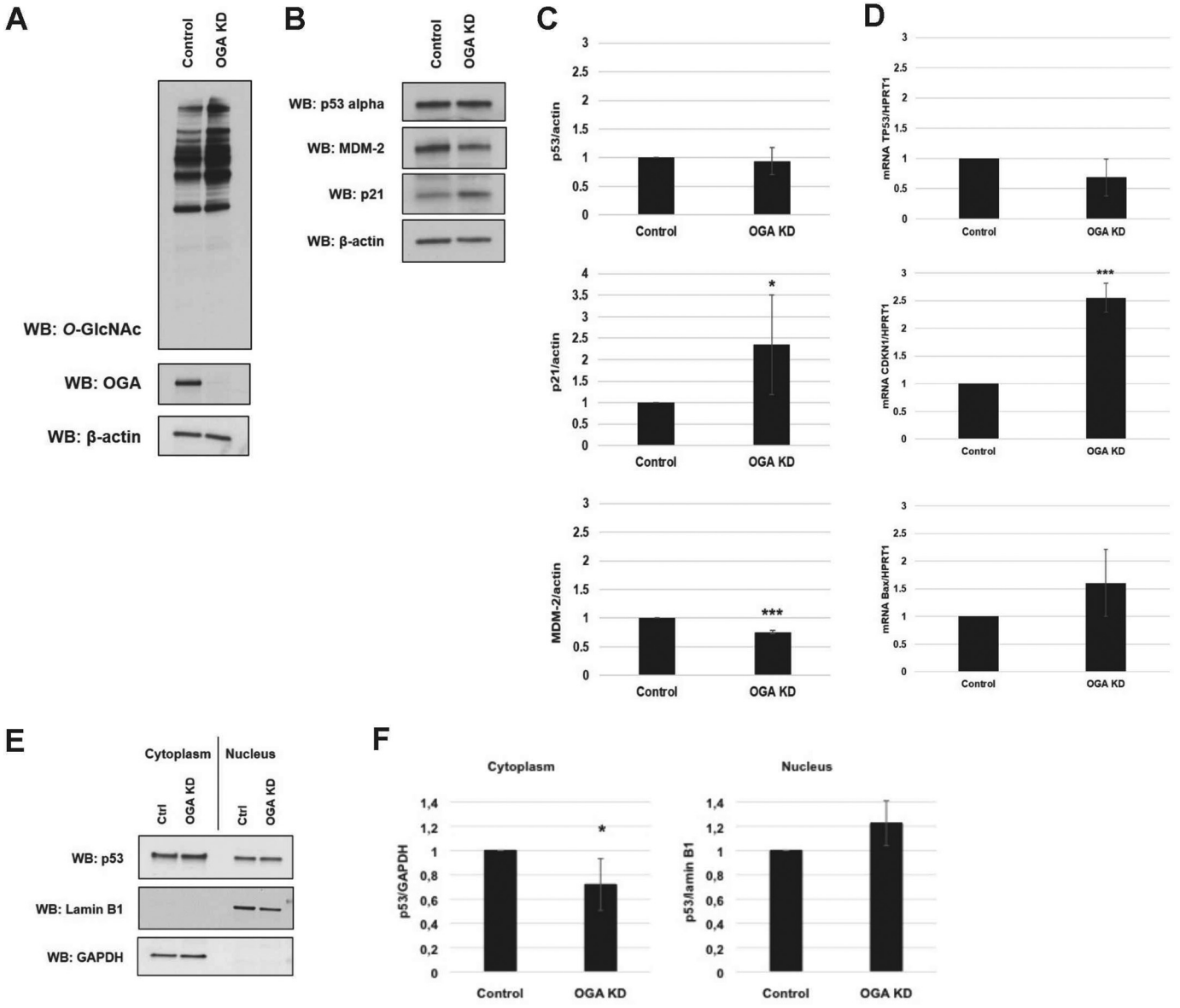

FIGURE 5. **Silencing of OGA increases wild type p53 function and alters its localization.** *A, O*-GlcNAc and OGA were measured by immunoblot. *B,* MDM-2, p53, and p21 protein levels were measured in knockdown cells by immunoblot. Actin was used as loading control. *C,* densitometry of protein expression in A2780 was normalized to actin levels. *D,* mRNA levels of p53, p21, and Bax in A2780 OGA knockdown cells were measured by qPCR. Cytoplasmic and nuclear preparations were made from control or silenced A2780 cells. *E,* p53 protein levels were measured by immunoblot, and GAPDH was used as loading control for cytoplasmic fractions, and lamin B1 was used as a loading control for nuclear fractions. *F,* densitometry of p53 expression in cytoplasmic and nuclear preparations normalized to GAPDH levels in cytoplasmic fractions and to lamin B1 levels in nuclear fractions. The mRNA levels of genes of interest were measured and normalized to HPRT1 mRNA levels. Protein and mRNA levels from OGA knockdown cells were normalized to control (pLKO) cells. All experiments were performed with at least three biological replicates. *, $p < 0.05$; **, $p < 0.01$; ***, $p < 0.0001$; *WB*, Western blotting.

could modulate the activity of these enzymes or their interactions with wild type p53. Acetylation of Lys-382 is important for recruitment of p300 to p21 promoter and for p21 expression by p53 (47), which corroborates the increase in p21 levels after OGT overexpression and OGA silencing. Granted, more experiments are needed to define how p53 acetylation is regulated by *O*-GlcNAc.

O-GlcNAcylation of Ser-149 and acetylation of Lys-382 are both PTMs that positively regulate p53 function. In contrast, phosphorylation of MDM-2 at Ser-166 prevents

FIGURE 4. **Pharmacological modulation of OGA increases p53 function and alters its localization in p53 wild type cells but not in p53-mutated cells.** Cancer cell lines were treated with the OGA inhibitor, TMG (10 μM), for 6 or 24 h. *O*-GlcNAcylation, MDM-2, and p53 (*A*) and p21 protein levels in TMG treatment (*B*) were measured by immunoblot, and actin was used as loading control. p53 (*C*) and p21 and Bax (*D*) mRNA levels after TMG treatment were measured and normalized to HPRT1 mRNA levels. Cytoplasmic and nuclear preparations of A2780 and OVCAR-8 were made after 6 h of TMG treatment. *E* and *G,* p53 protein levels were measured by immunoblotting; GAPDH was used as loading control for cytoplasmic fractions, and lamin B1 was used as loading control for nuclear fractions. *F* and *H,* densitometry of p53 expression in cytoplasmic and nuclear preparations normalized to GAPDH levels for cytoplasmic fractions and to lamin B1 levels in nuclear fractions. All experiments were performed with at least three biological replicates. *, $p < 0.05$; **, $p < 0.01$; ***, $p < 0.0001$; *WB*, Western blotting.

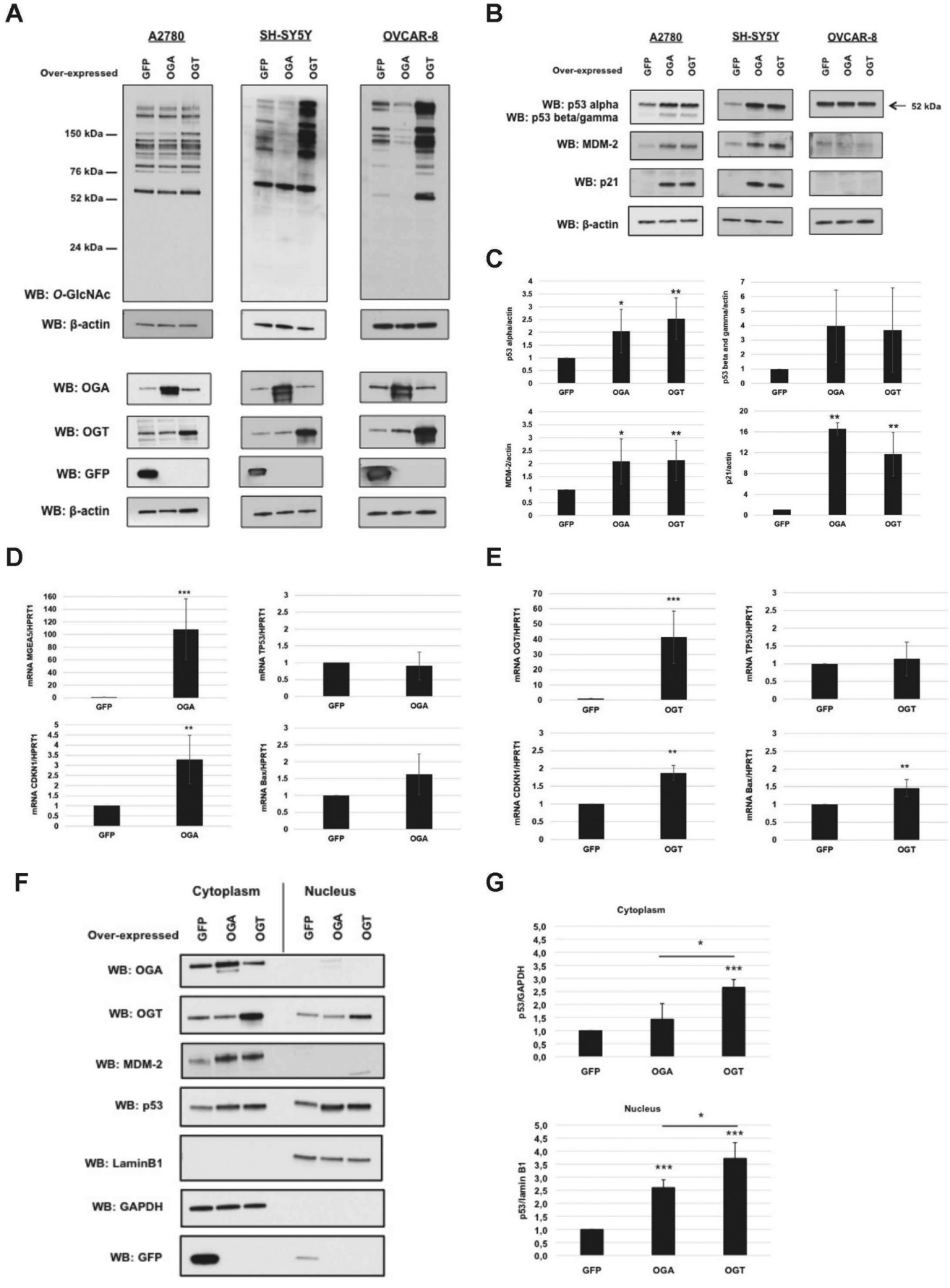
A
A2780
SH-SY5Y
OVCAR-8
Over-expressed
GFP
OGA
OGT
150 kDa
76 kDa
52 kDa
24 kDa
WB: O-GlcNAc
WB: β-actin
WB: OGA
WB: OGT
WB: GFP
WB: β-actin
B
WB: p53 alpha
WB: p53 beta/gamma
52 kDa
WB: MDM-2
WB: p21
WB: β-actin
C
p53 alpha/actin
p53 beta and gamma/actin
MDM-2/actin
p21/actin
D
mRNA MGEA5/HPRT1
mRNA TP53/HPRT1
mRNA CDKN1/HPRT1
mRNA Bax/HPRT1
E
mRNA OGT/HPRT1
mRNA TP53/HPRT1
mRNA CDKN1/HPRT1
mRNA Bax/HPRT1
F
Cytoplasm
Nucleus
WB: OGA
WB: OGT
WB: MDM-2
WB: p53
WB: LaminB1
WB: GAPDH
WB: GFP
G
Cytoplasm
p53/GAPDH
Nucleus
p53/lamin B1

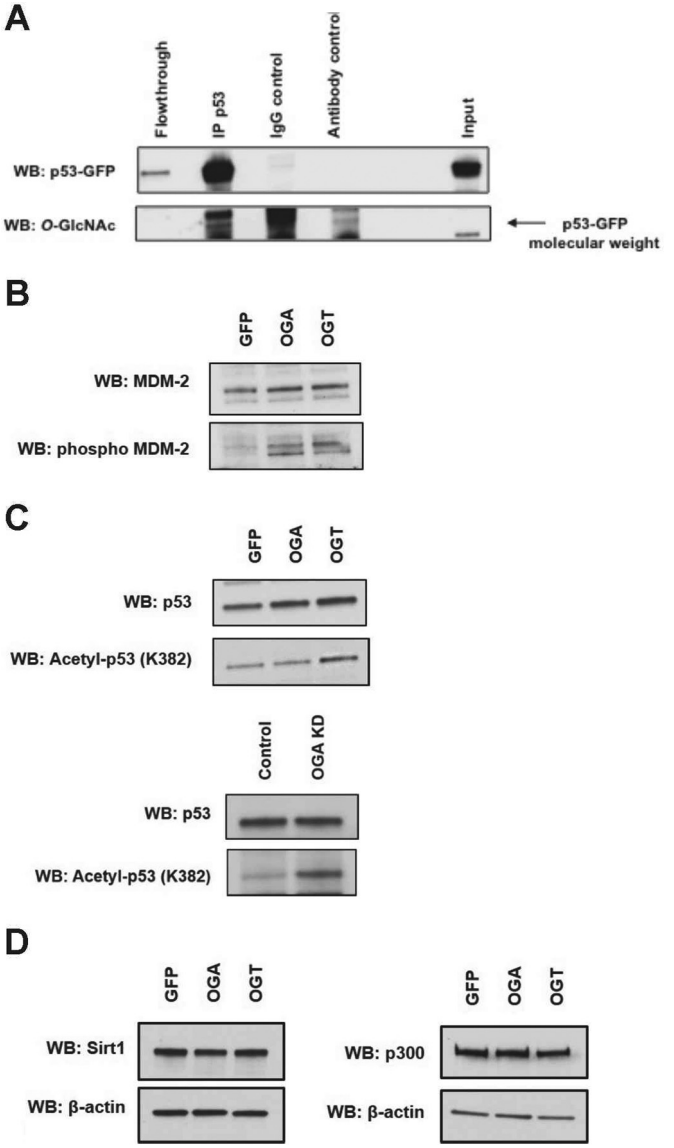

FIGURE 7. **Influence of *O*-GlcNAc modulation on PTMs in p53 pathway.** A2780 cells overexpressing GFP-p53 fusion protein were treated with TMG (10 μM) for 4 h. *A,* immunoprecipitated GFP-p53 was blotted against *O*-GlcNAc and p53. No *O*-GlcNAcylation was found on the tagged p53. *B,* MDM-2 and phospho-MDM-2 (Ser-166) levels were analyzed by immunoblot from A2780 cells overexpressing GFP, OGA, or OGT. *C,* p53 and acetyl-p53 (K382) proteins levels were analyzed by immunoblot from A2780 cells overexpressing GFP, OGA, or OGT and from A2780 OGA knockdown cells. *D,* Sirt1 and p300 protein levels were measured by immunoblotting from A2780 cells overexpressing GFP, OGA, or OGT, and actin was used as a loading control. All experiments were performed with at least three biological replicates. *, $p < 0.05$; **, $p < 0.01$; ***, $p < 0.0001$; *WB*, Western blotting.

MDM-2 degradation (29) leading to accumulation of MDM-2 and p53 degradation in the cytoplasm. In fact, activation of the p53 pathway is controlled by p53 up-regulation of the MDM-2 promoter. This self-regulatory feedback loop occurs in cells upon activation of the p53 pathway (48). The negative regulation induced by p53 activation acts as a form of control against overactivation of the pathway. Alterations to *O*-GlcNAc homeostasis increased phosphorylation of Ser-166 and MDM-2 levels suggesting that changes in cellular *O*-GlcNAc levels increase MDM-2 activation. However, this feedback loop is not sufficient to block the activation of the p53 pathway triggered by disruption in *O*-GlcNAc homeostasis.

The aim of the majority of chemotherapeutic agents in cancer therapy is to induce programmed cell death in tumor cells. The chemotherapeutic agent cisplatin alkylates DNA leading to considerable DNA damage, activation of the p53 pathway, and apoptosis (9). When we combined cisplatin with TMG, we observed a significant decrease in clonogenic growth. The combined treatments also increased G_2/M arrest. Interestingly, TMG alone did not interfere with cell growth, cell cycle progression, or cell death suggesting that the activation of p53 caused by TMG is not enough to induce significant effects on cell growth or cell death.

Although activation of the p53 pathway was increased with cisplatin and TMG treatment, colony formation assays using A2780 cells with silenced p53 also showed a trend toward decreased growth. These data indicate that the TMG/cisplatin effect on growth was partially dependent on p53 activation. TMG treatment might be regulating other growth-related pathways contributing to the decrease of colony formation observed with the TMG and cisplatin combination treatment. Importantly, tumors, and especially ovarian cancer, present a high rate of mutations of the p53 gene (27) that lead to loss of p53 tumor suppressor function. Thus, the fact that TMG treatment does not need functional p53 to affect cell growth (Fig. 10) would increase the range of tumors where combination therapy might enhance the efficacy of the chemotherapeutic. Interestingly, prolonged treatment with an OGA inhibitor (more than 3 months) increased *O*-GlcNAc levels in all tissues with no toxicity in mice (28). Potentially, OGA inhibition could be applicable as a drug target to control tumor growth without severe side effects toward healthy tissue. Hence, the use of OGA inhibitors as adjuvant therapy for cancer treatment might have minimal toxicity to normal tissues while enhancing the activity of the chemotherapeutic.

In conclusion, we showed that disruptions in *O*-GlcNAc homeostasis activate wild type p53 suggesting a model in which p53 senses cellular *O*-GlcNAc levels. Once *O*-GlcNAc homeostatic levels change, p53 becomes stabilized and moves into the nucleus. Nuclear translocation increases p53 acetylation and its

FIGURE 6. **OGA and OGT overexpression increases wild type p53 levels and function and alters its localization.** *A,* overexpressions of GFP, OGA, and OGT in two wild type cancer cell lines (A2780 and SH-SY5Y) and one mutated cancer cell line (OVCAR-8) were performed. *O*-GlcNAc, OGA, OGT, and GFP protein levels were measured by immunoblot. *B,* MDM-2, p53, and p21 protein levels were measured in wild type and mutated cells by immunoblot. *C,* densitometry of protein expression in A2780 was normalized to actin levels. The mRNA levels of p53, p21, and Bax in A2780 cells overexpressing GFP and OGA (*D*) or OGT (*E*) were measured by qPCR. Cytoplasmic and nuclear preparations were made in A2780 cells overexpressing GFP, OGA, and OGT. *F,* OGA, OGT, MDM-2, p53, and GFP protein levels were measured by immunoblot, and GAPDH was used as loading control for cytoplasmic fractions, and lamin B1 was used as a loading control for nuclear fractions. *G,* densitometry of p53 expression in cytoplasmic and nuclear preparations were normalized to GAPDH levels in cytoplasmic fractions and to lamin B1 levels in nuclear fractions. The mRNA levels of genes of interest were measured and normalized to HPRT1 mRNA levels. Protein and mRNA levels from OGA and OGT overexpressing cells were normalized to GFP-overexpressing cells. All experiments were performed with at least three biological replicates. *, $p < 0.05$; **, $p < 0.01$; ***, $p < 0.0001$; *WB*, Western blotting.

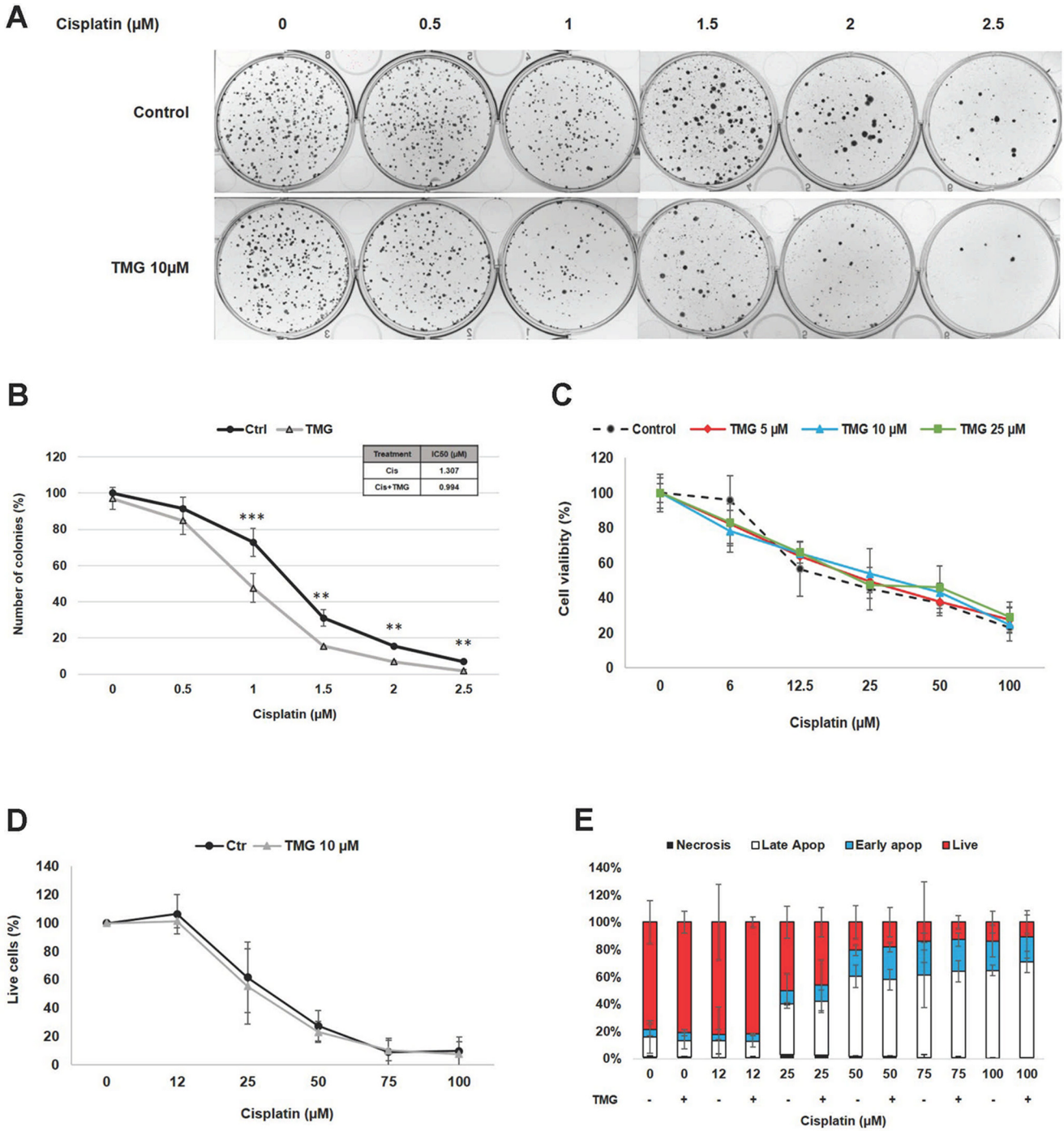

FIGURE 8. **TMG treatment alters growth but not cell death of A2780 cells during cisplatin treatment.** A2780 cells were pretreated with TMG (10 μM) or vehicle for 4 h followed by treatment with cisplatin for 24 h. *A,* colonies were counted 11 days later. *B,* colony formation was quantified between cisplatin (0.25–2 μM)-treated cells treated with or without TMG. *C,* MTT assays were performed with cells treated with cisplatin for 48 h (6–100 μM). Optical density normalized to untreated cells was considered 100%. *D* and *E,* cell death assay was performed with cells treated with cisplatin for 24 h (12–100 μM). Fluorescence intensity normalized to untreated cells was considered 100%. All experiments were performed with at least three biological replicates. *, $p < 0.05$; **, $p < 0.01$; ***, $p < 0.0001$.

affinity for DNA target sequences, resulting in increased transcription of p53 target genes like CDKN1 and BAX (Fig. 11), which in turn can induce cell cycle arrest or apoptosis. Thus, this work demonstrates that the wild type tumor suppressor p53 senses changes to *O*-GlcNAc homeostasis and suggests that using OGA inhibitors in association with cisplatin is beneficial for cancer treatment.

Experimental Procedures

Chemicals and Reagents—All primary and secondary antibodies used for immunoblotting were used at 1:1,000 and 1:10,000 dilution, respectively. Anti-*O*-linked *N*-acetylglucosamine antibody (RL2) (ab2739), anti-acetyl Lys-382 p53 (ab75754), and anti-GAPDH (ab9484) were purchased from Abcam. Antibodies for OGT (AL-34) and OGA (345) were gra-

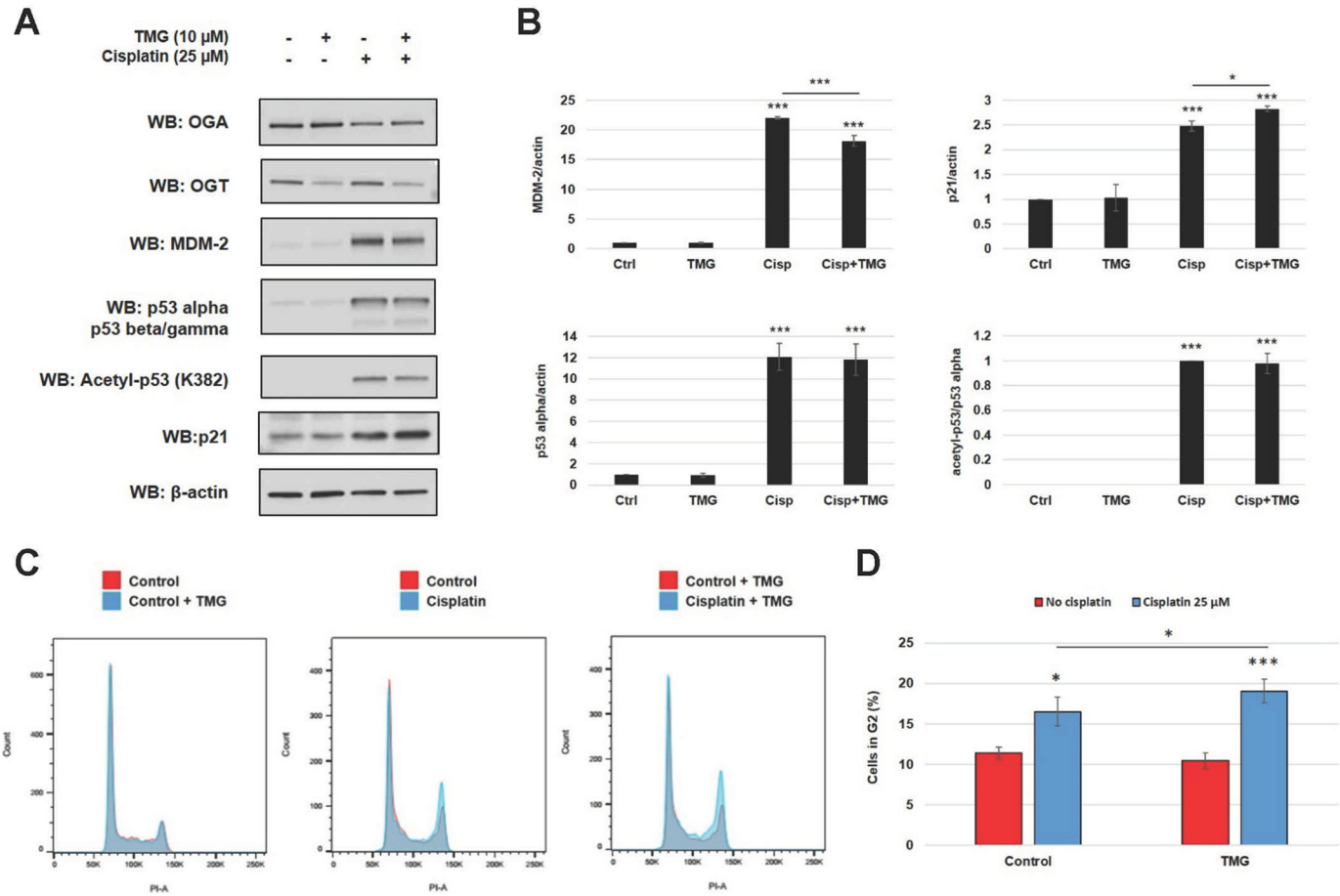

FIGURE 9. **TMG increases activation of p53 pathway and cell arrest in G_2/M during cisplatin treatment.** A2780 cells were pretreated with TMG (10 μM) or vehicle for 4 h followed by treatment with cisplatin (25 μM) for 24 h. *A*, OGA, OGT, MDM-2, p53, acetyl-p53 (Lys 382), and p21 protein levels were measured by immunoblot. *B*, protein levels were quantified and normalized to actin levels. *C*, cell cycle stage was measured by flow cytometry after TMG and cisplatin treatment. The plot is a representative histogram of fluorescence intensity after PI staining. *D*, percent of cells in G_2/M phase was calculated from each of the treatments. Actin was used as a loading control for immunoblotting. All experiments were performed with at least three biological replicates. *, $p < 0.05$; **, $p < 0.01$; ***, $p < 0.0001$; *WB*, Western blotting.

cious gifts from the Laboratory of Gerald Hart in the Department of Biological Chemistry at The Johns Hopkins University School of Medicine. Anti-β-actin (A2066), anti-α-tubulin (T5168), anti-OGA (SAB4200311), and anti-chicken IgY HRP (A9046) were purchased from Sigma. Anti-lamin B1 (D4Q4Z) (catalog no. 12586) and anti-SIRT1 (C14174) (catalog no. 2496) were purchased from Cell Signaling. Anti-MDM2 (SMP14) (sc-965), anti-p-MDM2 (Ser-166) (sc-293105), anti-p53 (DO-1) (sc-126), anti-p21 (F-5) (sc-6246), anti-p300 (C-20) (sc-585), and anti-green fluorescent protein (B-2) (sc-9996) were purchased from Santa Cruz Biotechnology. Anti-rabbit HRP (170-6515) and anti-mouse HRP (170-6516) were purchased from Bio-Rad. Nutlin-3 (N6287) and cisplatin (P4394) were purchased from Sigma. Thiamet-G (TMG) was purchased from SDChemMolecules.

Cell Culture—Human ovarian cancer cell lines A2780, SKOV-3, OVCAR-4, OVCAR-7, and OVCAR-10 were grown in 1:1 MCDB 105 medium and Medium 199 (M6395 and M4530, Sigma) supplemented with 5% heat-inactivated fetal bovine serum (FBS) (catalog no. 100-106, Gemini), 100 units of penicillin, and 100 mg/ml streptomycin (P433, Sigma), at 37 °C with 5% CO_2. Human ovarian cancer cell line OVCAR-8 was grown in RPMI 1640 medium (Sigma) supplemented with 5% heat-inactivated FBS, 100 units of penicillin, and 100 mg/ml streptomycin at 37 °C with 5% CO_2. The A2780 shRNA knockdown p53 cell lines (A2780shCtr, A2780sh#1, A2780sh#2, and A2780sh#3) were grown in 1:1 MCDB 105 medium and Medium 199 (Sigma) supplemented with 5% heat-inactivated FBS, 3 μg/ml puromycin (catalog no. 380-028-G001, Alexis Biochemicals), 100 units of penicillin, and 100 mg/ml streptomycin at 37 °C with 5% CO_2. Cells were subcultured using trypsin-EDTA (catalog no. 25200-056, Gibco) every 3 days. Human neuroblastoma cancer cell line SH-SY5Y was grown in Dulbecco's modified Eagle's Medium (DMEM) (Sigma) supplemented with 10% heat-inactivated FBS, 100 units of penicillin, and 100 mg/ml streptomycin at 37 °C with 5% CO_2. OGA, OGT (a kind gift from Gerald Hart, The Johns Hopkins University School of Medicine), and GFP (Baylor Vector Laboratories) adenovirus were used for infections for 48 h (multiplicity of infection of 25 for OVCAR-8, 50 for A2780, and 75 for SH-SY5Y). Lentiviral human OGA shRNA constructs 040 (RHS3979, Clone TRCN0000134040, Open Biosystems) was infected into ovarian cancer cell line A2780 using lentivirus media made in HEK293 cells and stable clones selected with puromycin (1 μg/ml). A2780 p53 silenced cell lines were generated by Chien and co-workers (49).

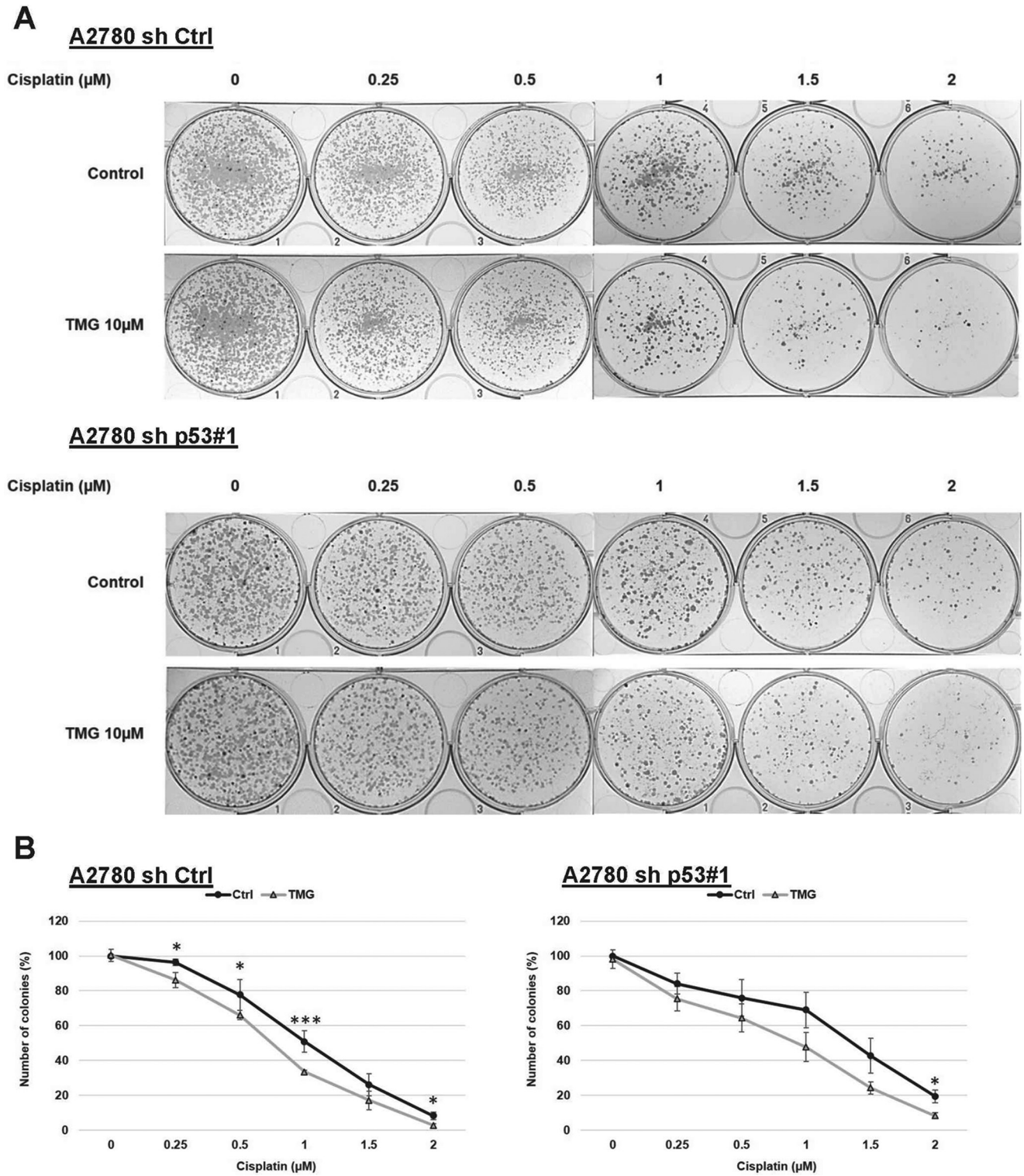

FIGURE 10. **Cell cycle arrest promoted by TMG in cisplatin treatment is partially dependent on p53.** A2780 cells were pretreated with TMG (10 μM) or vehicle for 4 h followed by treatment with cisplatin (0.25–2 μM) for 24 h. *A,* colony formation assay from A2780 p53 knockdown cells (A2780 sh p53#1) or control (A2780 shCtr) were performed. *B,* quantification of colony formation was normalized to untreated cells and considered 100%. All experiments were performed with at least three biological replicates. As a result of statistical analysis, *, $p < 0.05$; **, $p < 0.01$; ***, $p < 0.0001$.

Cytotoxicity Assay—Cell cytotoxicity was evaluated using MTT assay (M5655, Sigma) as described (50). Briefly, cells were seeded at a density of 1.5×10^4 cells/well in 96-well plate overnight, pretreated or not with 10 μM TMG for 4 h, and then exposed to various concentrations of cisplatin for 48 h. Four hours before the end of the treatment, cells were incubated with MTT (2.5 mg/ml) and kept in the dark at 37 °C until the end of the treatment. Formazan crystals produced by the reduction of MTT in the mitochondria by viable cells were dissolved in DMSO, and the optical density was measured with a plate

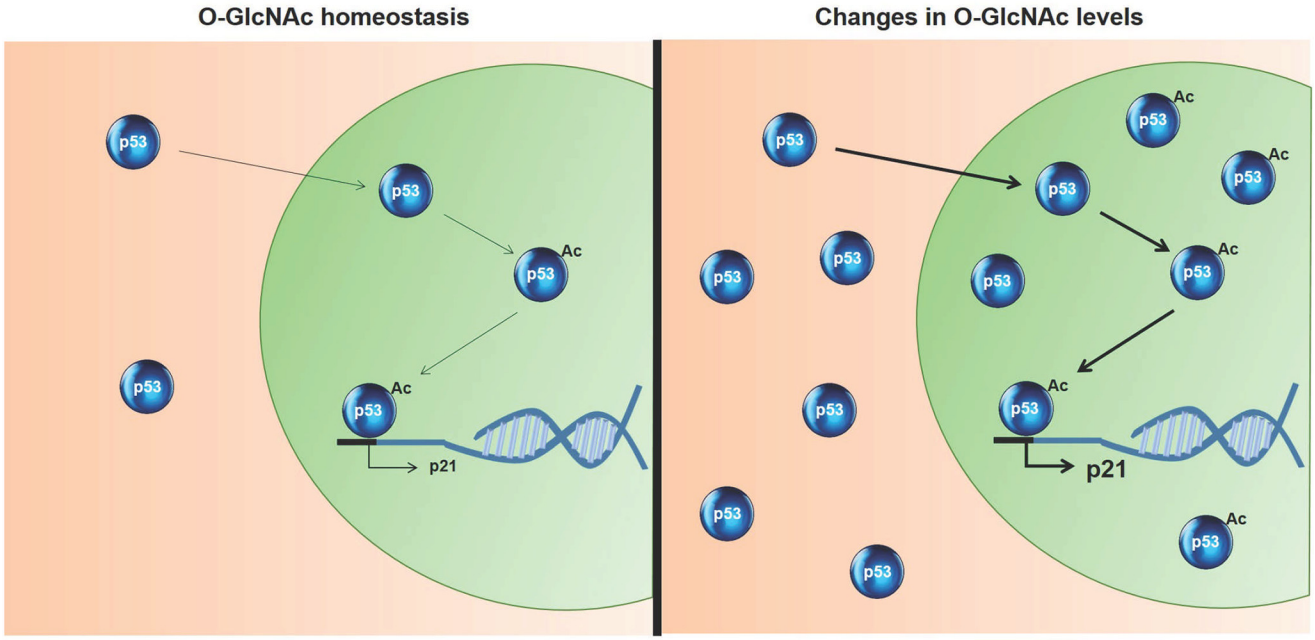

FIGURE 11. **Model of how p53 respond to changes in *O*-GlcNAc levels in cancer cells.** Changes in *O*-GlcNAc homeostasis increase p53 stabilization and translocation to the nucleus. Once in the nucleus, acetylation of p53 at Lys-382 is increased, and transcriptional activity of p53 is increased leading to gene expression of p53 target genes such as leading to p21 expression.

reader (Epoch, BioTek) at 570 nm (reference filter 630 nm). The results were expressed as percentage of the control, considered to be 100% ± S.D. DMSO was used as a vehicle control. Data were acquired and analyzed using Gen5 2.07 software.

Apoptotic Assay—Fluorescein annexin V-FITC/PI double labeling was performed with the annexin V-FITC apoptosis detection kit (catalog no. 4830-01-K, Trevigen). Ovarian cells were seeded in 24-well plates overnight (1×10^5 cells/well). Cells were pretreated with TMG (10 μM) or vehicle for 4 h and then exposed to various concentrations (12–100 μM) of cisplatin for 24 h. After treatment, cells were harvested and stained with annexin V-FITC and PI according to the manufacturer's instructions. The apoptotic cells were determined with a BD LSR II flow cytometer (BD Biosciences) and analyzed with BD FACSDiva software (BD Biosciences) at the University of Kansas Flow Cytometry Core.

Tumor Microarray Analysis—Tissue microarrays were constructed from archival formalin-fixed paraffin-embedded samples of ovarian carcinoma (48 patients) and primary peritoneal carcinoma (1 patient) along with matched metastases and recurrences (15 patients; 2 of these 15 patients had 2 recurrences each), matched metastases alone (27 patients), and matched recurrences alone (7 patients). These samples were identified from the pathology departmental archives of the University of Kansas Medical Center from 1998 to 2009. Based on review of the original pathology reports, the ovarian carcinomas were typed as serous (30 samples), mixed (14 samples; 12 of which included a serous component), carcinosarcoma (1 sample), clear cell (1 sample), papillary carcinoma (1), not otherwise specified (1 sample), and adenocarcinoma, not otherwise specified (1 sample), and the primary peritoneal carcinoma was also of the serous type. Normal samples were collected from the ovary and fallopian tube (9 samples). A board-certified pathologist selected tumor-rich areas after hematoxylin and eosin staining. Using the semi-automated TMArrayer (Pathology Devices, Inc., Westminster, MD), tissue microarrays paraffin blocks were assembled with triplicate 1.0-mm cores using the marked slide as a guide. The samples were subjected to staining for *O*-GlcNAcylation (RL-2 antibody, Abcam), OGT (AL-28), and OGA (SAB4200311, Sigma). A pathologist then scored the slides according to the intensity and localization of the staining.

Clonogenic Assay—Ovarian cells were seeded at 3,000 cells/well in 6-well plates overnight. Cells were either pretreated or not with TMG (10 μM) for 4 h and then exposed to various concentrations (0.5–2.5 μM) of cisplatin for 24 h. After treatment, wells were washed with PBS, and new media were replaced. Cells were maintained in culture for 11 days. Colonies formed after 11 days were stained with Crystal Violet (C3886, Sigma) and counted using ImageJ (National Institutes of Health).

Cell Cycle Analysis—Staining for DNA content by propidium iodide (catalog no. 195458, MP Biomedicals) was used to evaluate cell cycle phase. Twenty four hours after plating, cells (1×10^5 cells/well) were incubated with TMG (10 μM) for 4 h and then treated with cisplatin (30 μM) for 24 h. Next, the cells were harvested and resuspended in a hypotonic fluorescent solution (50 mg/ml PI and 0.1% Triton X-100 in 0.1% sodium citrate buffer) for 1 h in the dark at 4 °C. Cells were analyzed by flow cytometry (FL-2A) (BD LSR II, BD Biosciences). Data acquisition and analysis were controlled by BD FACSDiva software (BD Biosciences) (6).

Immunoblotting—Cells were lysed in lysis buffer (20 mM Tris, pH 7.4, 1% Nonidet P-40, 2 mM EDTA, 1 mM DTT, 40 mM *N*-acetylglucosamine, 150 mM NaCl, and protease inhibitors added at the time of preparation). Samples were loaded in equal protein amounts and fractionated by 4–15% polyacrylamide gradient gel (catalog no. 567-1084, Criterion Gels, Bio-Rad).

TABLE 2
Primer list

Gene	Forward primer	Reverse primer
TP53	5′-CATGAGCGCTGCTCAGATAG-3′	5′-TGGTACAGTCAGAGCCAACCT-3′
CDKN1	5′-GCAGACCAGCATGACAGATTT-3′	5′-GGATTAGGGCTTCCTCTTGGA-3′
BAX	5′-CCTGTGCACCAAGGTGCCGGAACT-3′	5′-CCACCCTGGTCTTGGATCCAGCCC-3′
MGEA5	5′-TTCACTGAAGGCTAATGGCTCCCG-3′	5′-ATGTCACAGGCTCCGACCAAGT-3′
OGT	5′-CATCGAGAATATCAGGCAGGAG-3′	5′-CCTTCGACACTGGAAGTGTATAG-3′
GFPT1	5′-CGG GAA AGT CAA GAT ACC AGC-3′	5′-CGT ACA CCA ATC AAC AGA GGG-3′
GFPT2	5′-GAT ACA GAG ACC ATC GCC AAG-3′	5′-GAC ACT CTT GAAAAC CAG CG-3′
HPRT1	5′-ATTGGTGGAGATGATCTCTCAACTTT-3′	5′-GCCAGTGTCAATTATATCTTCCACAA-3′

Proteins were transferred to a PVDF membrane (IPVH00010, Immobilon, Millipore) and blocked for 1 h with Tris-buffered saline containing 0.05% Tween 20 and 5% bovine serum albumin (BSA, catalog no. 50-753-3053, Fisher). Membranes were incubated overnight at 4 °C with primary antibody. Following a series of washes with Tris-buffered saline, 0.05% Tween 20, secondary horseradish peroxidase-conjugated antibody was added and incubated for 1 h at room temperature. After washing (five times for 5 min), the blot was visualized by chemiluminescence detection using chemiluminescent horseradish peroxidase reagent HyGlo (E2400, Denville Scientific) according to the manufacturer's instructions.

Immunoprecipitation—Cells were lysed in lysis buffer as before. Samples (1 mg of protein) were incubated with primary antibody or IgG control antibody overnight at 4 °C with constant rotation. The next day lysates were incubated with protein G-agarose beads (Millipore, catalog no. 16-266) at 4 °C with constant rotation for 2 h. Beads were washed five times with lysis buffer, and samples were used in immunoblotting.

Quantitative Real Time PCR (qPCR)—Total RNA was isolated by TRI reagent solution (AM9738, Ambion) according to the manufacturer's instruction. Briefly, cells were plated, harvested, and resuspended in 1 ml of TRI reagent solution followed by extraction with chloroform (T9424, Sigma). RNA was precipitated with isopropyl alcohol (UN1219, Fisher) by centrifugation, washed with 70% ethanol, and dissolved in nuclease-free water (AM9906, Ambion). A total of 1 μg of RNA was used for reverse transcription (RT) using iScript Reverse Transcription Supermix (170-8841, Bio-Rad). The cDNA products were diluted (1:10) with nuclease-free water and analyzed by qPCR using SsoAdvanced Universal SYBR Green Supermix (172-5271, Bio-Rad) according to the manufacturer's instruction. Briefly, cDNA, SYBR Green, nuclease-free water, and primers (Table 2) were mixed and added to a 96-well PCR plate (AVRT-LP, Midsci). Quantitative PCR analysis was performed using a CFX96 touch real time PCR detection system (185-5195, Bio-Rad) with the following protocol: polymerase activation and DNA denaturation for 30 s at 95 °C; amplification denaturation for 5 s at 95 °C and annealing for 30 s at 60 or 62 °C with 40 cycles; and melt curve 65–95 °C with 0.5 °C increment 5 s/step. Quantification cycle (C_q) value was recorded by CFX Manager™ software.

Subcellular Fractionation—After harvesting and pelleting, cells were resuspended in hypotonic buffer (20 mM HEPES, pH 7.5, 50 mM NaF, 5 mM $Na_2P_2O_7$, 50 mM *N*-acetylglucosamine, 1 mM EDTA, 1 mM EGTA, 1 mM DTT, 1 mM PMSF and protease inhibitor mixture) and centrifuged. The supernatant was saved (cytoplasmic fraction), and the pellet was washed 10 times with hypotonic buffer. After washing, the pellet was lysed with Nonidet P-40 lysis buffer and centrifuged for 20 min at 20,000 × *g*; the resulting supernatant was the nuclear fraction. The protein levels in the fractions were analyzed by immunoblotting and normalized by lamin B1 levels for nuclear fraction and by GAPDH for cytoplasmic fraction.

Statistical Analysis—All the data reported in this paper were expressed as the mean ± S.D. from at least three independent experiments. A significant difference from the respective control for each experimental test condition was assessed by one-way analysis of variance or Student's *t* test using GraphPad Prism 6.0 software. Values of $p < 0.05$ were considered statistically significant.

Author Contributions—R. M. Q. conducted the experiments, analyzed the results, and wrote the paper. R. M. scored the tumor microarray samples. R. M. Q., J. C., W. B. D., and C. S. conceived the idea for the project and contributed to manuscript preparation. All authors reviewed the results and approved the final version of the manuscript.

Acknowledgments—Biospecimen Core Resources was recipient of NCI Cancer Center Support Grant P30 CA168524 from the National Institutes of Health.

References

1. Hart, G. W. (1997) Dynamic *O*-linked glycosylation of nuclear and cytoskeletal proteins. *Annu. Rev. Biochem.* **66,** 315–335
2. Dias, W. B., Cheung, W. D., and Hart, G. W. (2012) *O*-GlcNAcylation of kinases. *Biochem. Biophys. Res. Commun.* **422,** 224–228
3. de Queiroz, R. M., Carvalho, E., and Dias, W. B. (2014) *O*-GlcNAcylation: the sweet side of the cancer. *Front. Oncol.* **4,** 132
4. Hart, G. W., Slawson, C., Ramirez-Correa, G., and Lagerlof, O. (2011) Cross-talk between *O*-GlcNAcylation and phosphorylation: roles in signaling, transcription, and chronic disease. *Annu. Rev. Biochem.* **80,** 825–858
5. Shafi, R., Iyer, S. P., Ellies, L. G., O'Donnell, N., Marek, K. W., Chui, D., Hart, G. W., and Marth, J. D. (2000) The *O*-GlcNAc transferase gene resides on the X chromosome and is essential for embryonic stem cell viability and mouse ontogeny. *Proc. Natl. Acad. Sci. U.S.A.* **97,** 5735–5739
6. Slawson, C., Zachara, N. E., Vosseller, K., Cheung, W. D., Lane, M. D., and Hart, G. W. (2005) Perturbations in *O*-linked β-*N*-acetylglucosamine protein modification cause severe defects in mitotic progression and cytokinesis. *J. Biol. Chem.* **280,** 32944–32956
7. Dias, W. B., Cheung, W. D., Wang, Z., and Hart, G. W. (2009) Regulation of calcium/calmodulin-dependent kinase IV by *O*-GlcNAc modification. *J. Biol. Chem.* **284,** 21327–21337
8. Gewinner, C., Hart, G., Zachara, N., Cole, R., Beisenherz-Huss, C., and Groner, B. (2004) The coactivator of transcription CREB-binding protein interacts preferentially with the glycosylated form of Stat5. *J. Biol. Chem.* **279,** 3563–3572

9. Peternelj, T. T., Marsh, S. A., Strobel, N. A., Matsumoto, A., Briskey, D., Dalbo, V. J., Tucker, P. S., and Coombes, J. S. (2015) Glutathione depletion and acute exercise increase *O*-GlcNAc protein modification in rat skeletal muscle. *Mol. Cell. Biochem.* **400,** 265–275
10. Groves, J. A., Lee, A., Yildirir, G., and Zachara, N. E. (2013) Dynamic *O*-GlcNAcylation and its roles in the cellular stress response and homeostasis. *Cell Stress Chaperones* **18,** 535–558
11. Bond, M. R., and Hanover, J. A. (2015) A little sugar goes a long way: The cell biology of *O*-GlcNAc. *J. Cell Biol.* **208,** 869–880
12. Warburg, O. (1956) Origin of cancer cells. *Science* **123,** 309–314
13. Vasconcelos-dos-Santos, A., Oliveira, I. A., Lucena, M. C., Mantuano, N. R., Whelan, S. A., Dias, W. B., and Todeschini, A. R. (2015) Biosynthetic machinery involved in aberrant glycosylation: promising targets for developing of drugs against cancer. *Front. Oncol.* **5,** 138
14. Itkonen, H. M., Minner, S., Guldvik, I. J., Sandmann, M. J., Tsourlakis, M. C., Berge, V., Svindland, A., Schlomm, T., and Mills, I. G. (2013) *O*-GlcNAc transferase integrates metabolic pathways to regulate the stability of c-MYC in human prostate cancer cells. *Cancer Res.* **73,** 5277–5287
15. Marshall, S., Nadeau, O., and Yamasaki, K. (2004) Dynamic actions of glucose and glucosamine on hexosamine biosynthesis in isolated adipocytes: differential effects on glucosamine 6-phosphate, UDP-*N*-acetylglucosamine, and ATP levels. *J. Biol. Chem.* **279,** 35313–35319
16. Mi, W., Gu, Y., Han, C., Liu, H., Fan, Q., Zhang, X., Cong, Q., and Yu, W. (2011) *O*-GlcNAcylation is a novel regulator of lung and colon cancer malignancy. *Biochim. Biophys. Acta* **1812,** 514–519
17. Krzeslak, A., Pomorski, L., and Lipinska, A. (2010) Elevation of nucleocytoplasmic β-*N*-acetylglucosaminidase (*O*-GlcNAcase) activity in thyroid cancers. *Int. J. Mol. Med.* **25,** 643–648
18. Shi, Y., Tomic, J., Wen, F., Shaha, S., Bahlo, A., Harrison, R., Dennis, J. W., Williams, R., Gross, B. J., Walker, S., Zuccolo, J., Deans, J. P., Hart, G. W., and Spaner, D. E. (2010) Aberrant *O*-GlcNAcylation characterizes chronic lymphocytic leukemia. *Leukemia* **24,** 1588–1598
19. Lynch, T. P., Ferrer, C. M., Jackson, S. R., Shahriari, K. S., Vosseller, K., and Reginato, M. J. (2012) Critical role of *O*-linked β-*N*-acetylglucosamine transferase in prostate cancer invasion, angiogenesis, and metastasis. *J. Biol. Chem.* **287,** 11070–11081
20. Ma, Z., and Vosseller, K. (2013) *O*-GlcNAc in cancer biology. *Amino Acids* **45,** 719–733
21. Bieging, K. T., and Attardi, L. D. (2012) Deconstructing p53 transcriptional networks in tumor suppression. *Trends Cell Biol.* **22,** 97–106
22. Shi, D., and Gu, W. (2012) Dual roles of MDM2 in the regulation of p53: ubiquitination dependent and ubiquitination independent mechanisms of MDM2 repression of p53 activity. *Genes Cancer* **3,** 240–248
23. Gu, B., and Zhu, W. G. (2012) Surf the post-translational modification network of p53 regulation. *Int. J. Biol. Sci.* **8,** 672–684
24. Wang, X., Simpson, E. R., and Brown, K. A. (2015) p53: protection against tumor growth beyond effects on cell cycle and apoptosis. *Cancer Res.* **75,** 5001–5007
25. Wattel, E., Preudhomme, C., Hecquet, B., Vanrumbeke, M., Quesnel, B., Dervite, I., Morel, P., and Fenaux, P. (1994) p53 mutations are associated with resistance to chemotherapy and short survival in hematologic malignancies. *Blood* **84,** 3148–3157
26. Yang, W. H., Kim, J. E., Nam, H. W., Ju, J. W., Kim, H. S., Kim, Y. S., and Cho, J. W. (2006) Modification of p53 with *O*-linked *N*-acetylglucosamine regulates p53 activity and stability. *Nat. Cell Biol.* **8,** 1074–1083
27. Schuijer, M., and Berns, E. M. (2003) TP53 and ovarian cancer. *Hum. Mutat.* **21,** 285–291
28. Macauley, M. S., Shan, X., Yuzwa, S. A., Gloster, T. M., and Vocadlo, D. J. (2010) Elevation of global O-GlcNAc in rodents using a selective *O*-GlcNAcase inhibitor does not cause insulin resistance or perturb glucohomeostasis. *Chem. Biol.* **17,** 949–958
29. Malmlöf, M., Roudier, E., Högberg, J., and Stenius, U. (2007) MEK-ERK-mediated phosphorylation of Mdm2 at Ser-166 in hepatocytes. Mdm2 is activated in response to inhibited Akt signaling. *J. Biol. Chem.* **282,** 2288–2296
30. Finlay, C. A., Hinds, P. W., and Levine, A. J. (1989) The p53 proto-oncogene can act as a suppressor of transformation. *Cell* **57,** 1083–1093
31. Venkatachalam, S., Tyner, S. D., Pickering, C. R., Boley, S., Recio, L., French, J. E., and Donehower, L. A. (2001) Is p53 haploinsufficient for tumor suppression? Implications for the p53+/− mouse model in carcinogenicity testing. *Toxicol. Pathol.* **29,** 147–154
32. Malaguarnera, R., Vella, V., Vigneri, R., and Frasca, F. (2007) p53 family proteins in thyroid cancer. *Endocr. Relat. Cancer* **14,** 43–60
33. Wang, T., Birsoy, K., Hughes, N. W., Krupczak, K. M., Post, Y., Wei, J. J., Lander, E. S., and Sabatini, D. M. (2015) Identification and characterization of essential genes in the human genome. *Science* **350,** 1096–1101
34. O'Donnell, N., Zachara, N. E., Hart, G. W., and Marth, J. D. (2004) Ogt-dependent X-chromosome-linked protein glycosylation is a requisite modification in somatic cell function and embryo viability. *Mol. Cell. Biol.* **24,** 1680–1690
35. Dashzeveg, N., and Yoshida, K. (2015) Cell death decision by p53 via control of the mitochondrial membrane. *Cancer Lett.* **367,** 108–112
36. Tasdemir, E., Maiuri, M. C., Galluzzi, L., Vitale, I., Djavaheri-Mergny, M., D'Amelio, M., Criollo, A., Morselli, E., Zhu, C., Harper, F., Nannmark, U., Samara, C., Pinton, P., Vicencio, J. M., Carnuccio, R., *et al.* (2008) Regulation of autophagy by cytoplasmic p53. *Nat. Cell Biol.* **10,** 676–687
37. Issaeva, N., Bozko, P., Enge, M., Protopopova, M., Verhoef, L. G., Masucci, M., Pramanik, A., and Selivanova, G. (2004) Small molecule RITA binds to p53, blocks p53-HDM-2 interaction and activates p53 function in tumors. *Nat. Med.* **10,** 1321–1328
38. Van Maerken, T., Rihani, A., Van Goethem, A., De Paepe, A., Speleman, F., and Vandesompele, J. (2014) Pharmacologic activation of wild type p53 by nutlin therapy in childhood cancer. *Cancer Lett.* **344,** 157–165
39. Gurel, Z., Zaro, B. W., Pratt, M. R., and Sheibani, N. (2014) Identification of *O*-GlcNAc modification targets in mouse retinal pericytes: implication of p53 in pathogenesis of diabetic retinopathy. *PLoS One* **9,** e95561
40. Marsh, S. A., Dell'Italia, L. J., and Chatham, J. C. (2011) Activation of the hexosamine biosynthesis pathway and protein *O*-GlcNAcylation modulate hypertrophic and cell signaling pathways in cardiomyocytes from diabetic mice. *Amino Acids* **40,** 819–828
41. Zhong, J., Martinez, M., Sengupta, S., Lee, A., Wu, X., Chaerkady, R., Chatterjee, A., O'Meally, R. N., Cole, R. N., Pandey, A., and Zachara, N. E. (2015) Quantitative phosphoproteomics reveals crosstalk between phosphorylation and *O*-GlcNAc in the DNA damage response pathway. *Proteomics* **15,** 591–607
42. Muller, P. A., and Vousden, K. H. (2014) Mutant p53 in cancer: new functions and therapeutic opportunities. *Cancer Cell* **25,** 304–317
43. Hardivillé, S., and Hart, G. W. (2014) Nutrient regulation of signaling, transcription, and cell physiology by *O*-GlcNAcylation. *Cell Metab.* **20,** 208–213
44. Peternelj, T. T., Marsh, S. A., Morais, C., Small, D. M., Dalbo, V. J., Tucker, P. S., and Coombes, J. S. (2015) *O*-GlcNAc protein modification in C2C12 myoblasts exposed to oxidative stress indicates parallels with endogenous antioxidant defense. *Biochem. Cell Biol.* **93,** 63–73
45. Zhang, E., Guo, Q., Gao, H., Xu, R., Teng, S., and Wu, Y. (2015) Metformin and resveratrol inhibited high glucose-induced metabolic memory of endothelial senescence through SIRT1/p300/p53/p21 pathway. *PloS one* **10,** e0143814
46. Dai, C., and Gu, W. (2010) p53 post-translational modification: deregulated in tumorigenesis. *Trends Mol. Med.* **16,** 528–536
47. Zhao, Y., Lu, S., Wu, L., Chai, G., Wang, H., Chen, Y., Sun, J., Yu, Y., Zhou, W., Zheng, Q., Wu, M., Otterson, G. A., and Zhu, W. G. (2006) Acetylation of p53 at lysine 373/382 by the histone deacetylase inhibitor depsipeptide induces expression of p21(Waf1/Cip1). *Mol. Cell. Biol.* **26,** 2782–2790
48. Zhang, C., Liu, J., Wang, X., and Feng, Z. (2015) The regulation of the p53/MDM2 feedback loop by microRNAs. *RNA Dis.* **2,** e502
49. Zhang, X., Cheng, L., Minn, K., Madan, R., Godwin, A. K., Shridhar, V., and Chien, J. (2014) Targeting of mutant p53-induced FoxM1 with thiostrepton induces cytotoxicity and enhances carboplatin sensitivity in cancer cells. *Oncotarget* **5,** 11365–11380
50. Queiroz, R. M., Takiya, C. M., Guimarães, L. P., Rocha Gda, G., Alviano,

D. S., Blank, A. F., Alviano, C. S., and Gattass, C. R. (2014) Apoptosis-inducing effects of *Melissa officinalis* L. essential oil in glioblastoma multiforme cells. *Cancer Invest.* **32,** 226–235

51. Anglesio, M. S., Wiegand, K. C., Melnyk, N., Chow, C., Salamanca, C., Prentice, L. M., Senz, J., Yang, W., Spillman, M. A., Cochrane, D. R., Shumansky, K., Shah, S. P., Kalloger, S. E., and Huntsman, D. G. (2013) Specific cell line models for type-specific ovarian cancer research. *PLoS One* 10.1371/journal.pone.0072162
52. Zhang, X., Cheng, L., Minn, K., Madan, R., Godwin, A. K., Shridhar, V., and Chien, J. (2014) Targeting of mutant p53-induced FoxM1 with thiostrepton induces cytotoxicity and enhances carboplatin sensitivity in cancer cells. *Oncotarget* **5,** 11365–11380